

Dynamics of short-term ecosystem carbon fluxes induced by precipitation events in a semiarid grassland.

Josué Delgado-Balbuena¹, Henry W. Loescher^{2,3}, Carlos A. Aguirre-Gutiérrez¹, Teresa Alfaro-Reyna¹, Luis F. Pineda-Martínez⁴, Rodrigo Vargas⁵, and ~~José T. Tulio~~ Arredondo⁶.

¹Centro Nacional de Investigación Disciplinaria Agricultura Familiar, INIFAP, km 8.5 Carr. Ojuelos – Lagos de Moreno, 47563, Ojuelos de Jalisco, Jal., México

²Battelle, National Ecological Observatory Network (NEON), Boulder, CO USA 80301,

³Institute of Alpine and Arctic Research (INSTAAR), University of Colorado, Boulder, CO USA 80301.

⁴Universidad Autónoma de Zacatecas, 108 Calzada Universidad, 98066 Zacatecas, Zacatecas, Mexico

⁵Department of Plant and Soil Sciences, University of Delaware, Newark, DE, USA

⁶Division de Ciencias Ambientales, Instituto Potosino de Investigación Científica y Tecnológica, Camino a la Presa de San José 2055, Lomas 4ta, 78216 San Luis Potosí, S.L.P., México.

Correspondence to: Josué Delgado-Balbuena (delgado.josue@inifap.gob.mx)

Abstract. ~~Precipitation~~ Infrequent and small PPT events characterize precipitation (PPT) patterns in semiarid grasslands ~~are characterized by infrequent and small PPT events~~; however, plants and soil microorganisms are adapted to use the unpredictable small pulses of water. Several studies have shown short-term responses of carbon and nitrogen mineralization rates (called the priming effect or the Birch effect) stimulated by wet-dry cycles; however, dynamics, drivers, and the contribution of the “priming effect” to the annual C balance ~~is~~ are poorly understood. Thus, we analysed six years of continuous net ecosystem exchange measurements to evaluate the effect of the PPT periodicity, and magnitude of individual PPT events on the daily/annual ecosystem C balance (NEE) in a semiarid grassland. We included the period between PPT events, a prioriprevious daytime NEE rate, and a prioriprevious soil moisture content as the main drivers of the priming effect. Ecosystem respiration (ER) responded within few hours following a PPT event, whereas it took five-nine days for gross ecosystem exchange (GEE; such as where $-NEE = GEE + ER$) to respond. Precipitation events as low as 0.25 mm increased ER, but cumulative PPT > 40 mm ~~that infiltrated~~ infiltrating deep into the soil profile stimulated GEE. Overall, ER fluxes following PPT events were related to the change of soil water content at shallow depth and previous soil conditions (e.g., previous NEE rate, previous soil water content) and the size of the stimulus (e.g., PPT event size). Carbon effluxes from the priming effect accounted for less than 5% of ecosystem respiration but were ~~significatively~~ significantly high respect to the carbon balance. In the long-term, changes in PPT regimes to more intense and less frequent PPT events, as expected by the effects of climate change ~~effect~~, could convert the semiarid grassland from a ~~slight~~ small C sink to a C source.

Keywords: Eddy covariance, net ecosystem exchange, ecosystem respiration, *Bouteloua gracilis*, blue grama, priming effect, Birch effect.

36 1. Introduction

37 Arid lands comprise ~~a wide range of many~~ ecosystem types covering more than 30% of terrestrial land (Lal,
38 2004). In these ecosystems annual potential evapotranspiration is larger than ~~annual/yearly~~ precipitation due to
39 regional atmospheric high-pressure zones (~~i.e.~~, Hadley cells), continental winds, cold oceanic winds and local
40 orographic effects that reduce the precipitation amounts (Maliva and Missimer, 2012). Here, precipitation (PPT)
41 occurs as infrequent, discrete, small (< 5 mm)~~),~~ and unpredictable events (Noy-Meir, 1973; Loik et al, 2004).
42 This results in water-limited ecosystems, where biological activity is restricted to periods of soil water
43 availability (Lauenroth and Sala, 1992). Consequently, the productivity and stability of these ecosystems are
44 more vulnerable to changes in climate, particularly to changes ~~of in~~ the historic mean annual PPT (~~MAP~~)
45 amounts (~~MAP~~; Wang et al., 2021) and the change in the periodicity (~~i.e.~~, frequency) of these PPT events-
46 (~~Korell et al., 2021; Nielsen and Ball, 2015~~).

47 Precipitation stimulates short-term changes of carbon and nitrogen mineralization rates because soil
48 microorganisms activate with ~~the increase of increased~~ soil water content (Turner and Haygarth, 2001). This
49 “priming effect” (Borken and Matzner, 2009)~~),~~ also called the Birch effect (Birch, 1964), describes the soil
50 carbon released from ~~the~~ decomposition of heterotrophic sources to the atmosphere following soil rewetting.
51 ~~Amount~~The amount and timing of PPT events modify the magnitude and duration of the priming effect by
52 modulating soil wet-dry cycles. The size of a PPT event determines the temporal duration and the biotic
53 components that respond to the pulse (Huxman et al., 2004a), ~~and thus, defines defining~~ the magnitude and
54 direction of CO₂ effluxes (Chen et al., 2009). In general, small precipitation events that induce changes in soil
55 humidity at shallow ~~depth~~depths do not induce plant activity, but activate soil microorganisms (Collins et al.,
56 2008) ~~and consequently enhance CO₂ effluxes (Vargas et al., 2012)~~. On the other hand, successive rewetting
57 cycles reduce carbon mineralization rates as the amount of available organic labile carbon declines (Jarvis et
58 al., 2007). Thus, PPT events after long drought periods (until nine months in semiarid ~~grasslands~~grassland)
59 trigger larger and longer soil respiration efflux rates ~~compared to than~~ consecutive PPT events (Reichmann et
60 al., 2013; Vargas et al., 2018).

61 At the ecosystem scale, deserts and grasslands have shown larger CO₂ efflux rates after rewetting than temperate
62 ecosystems or croplands (Kim et al., 2012)~~),~~ and in ecosystems with low soil organic carbon content (Bastida
63 et al., 2019). Characteristics and dynamics of these short-term soil C effluxes were addressed by the “Threshold-
64 Delay” model (T-D model, Ogle and Reynolds 2004). The T-D model ~~take the~~takes previous environmental
65 conditions, PPT event size, PPT thresholds, and time-delays to inform the time constants that modulate
66 ecosystem responses after a PPT event. Moreover, Huxman et al.~~.,~~ (2004a) described the dynamics of the net
67 ecosystem exchange of carbon (NEE) and its components (gross ecosystem exchange = GEE, and ecosystem
68 respiration = ER, such as -NEE = GEE + ER) with parameters of the T-D model (Fig. A1). GEE and ER have
69 different time delays based on threshold PPT quantities and event size, with ER responding to smaller PPT
70 events than GEE (Huxman et al. 2004a). In addition, ~~both~~ GEE and ER have asymptotic responses to large PPT
71 events (the upper PPT thresholds), with an upper ER threshold lower than that found for ~~the~~GEE ~~threshold~~
72 (Huxman et al. 2004).

73 In the semiarid grasslands of Mexico, small PPT events ~~are likely to~~ activate biological soil crusts (BSC) ~~on the~~
74 ~~soil surface~~ that cover up to 60% of plant interspaces (Concostrina-Zubiri et al., 2014), ~~and to~~ stimulate ER
75 instead of C uptake. However, *Bouteloua gracilis* H.B.K. Lag ex Steud (blue grama), the keystone species in
76 the semiarid grassland of Mexico (Medina-Roldán et al., 2007) may contribute to C uptake because of its
77 adaptations to take advantage of ~~smaller~~ small PPT events (Sala and Lauenroth, 1982, Medina-Roldán et al.,
78 2013). Understanding disturbances of ecosystem processes (C fluxes) due to changing regional PPT
79 ~~pattern~~ patterns in semiarid grasslands ~~is~~ are particularly salient given that the global circulation models forecast
80 ~~a~~ between 10% ~~to~~ and 30% reduction of summer and winter precipitation, respectively ~~at~~ by the end of the 21st
81 Century (Christensen et al., 2007), ~~and the~~. Furthermore, PPT patterns ~~is forecasted~~ are expected to have fewer
82 events with more water quantity per event (Easterling et al., 2000).

83 ~~Thus, the~~ The objective of this study was to evaluate the effect of PPT periodicity and magnitude of individual
84 PPT events and a priori soil moisture conditions on daily and annual ecosystem C balance (NEE) for the
85 semiarid grassland in Mexico. Over a six-year study period, we examined event-based PPT amount, the period
86 between PPT events, ~~a priori~~ and the previous daytime NEE rate and ~~a priori~~ soil water content at two depths as
87 the main drivers of daily mean NEE change rate. Because we were interested ~~on~~ in short-term NEE
88 ~~change~~ changes and ~~its~~ their components, only short-term NEE ~~change~~ changes within a few days following a
89 PPT event were evaluated. Effects on daily mean GEE (GEE = -NEE + ER) ~~was~~ were also evaluated at the
90 beginning of the growing season. Based on the T-D model (Ogle and Reynolds, 2004), we expect that; 1)
91 semiarid grassland will exhibit a quick response (short time-delay) to small PPT events (Low PPT threshold)
92 through positive NEE fluxes (C release, H1). Moreover, 2) ER and GEE (C release and C uptake, respectively)
93 will differ in their ~~time~~ response times and PPT thresholds, with shorter time-delays and lower PPT thresholds
94 for ER than GEE (H2). This response is because ~~of~~ small PPT events should enhance ER mainly through
95 heterotrophic respiration of soil surface microorganisms that are activated within one hour after wetting
96 (Placella et al., 2012), whereas larger PPT events are required to reach roots at deeper soil profiles and ~~that~~
97 ~~plants need~~ longer times for plants to start growing. On the other hand, we expect that; 3) the size and timing
98 of PPT patterns will modulate the magnitude of C efflux; therefore, large precipitation events after long dry
99 periods will release more CO₂ than small or consecutive PPT events (H3). Finally, we expect; 4) C efflux after
100 PPT events will be a meaningful CO₂ source to the atmosphere in the semiarid grassland ~~which will decrease,~~
101 ~~decreasing~~ the ecosystem's annual net C uptake ~~of the ecosystem~~ (H4).

102 2. Materials and methods

103 2.1 Site description

104 The study site is located on a shortgrass steppe, within the Llanos de Ojuelos subprovince of Jalisco state,
105 Mexico. The shortgrass biome in Mexico extends from the North American Midwest along a strip that follows
106 the Sierra Madre Occidental through the Chihuahuan Desert into the sub-province Llanos de Ojuelos.
107 Vegetation is dominated by grasses, with *Bouteloua gracilis* (Willd. ex Kunth) Lag. ex ~~Griffiths~~ Griffiths as
108 the key grass species, forming near mono-specific stands. The region has a semiarid climate with mean annual

109 precipitation of 424 mm \pm 11 mm (last 30 years, Delgado-Balbuena et al., 2019) distributed mainly between
110 June and September and with 6 to 9 months of no-rain/low PPT. Winter-summer rain accounts for <
111 20% of the total annual precipitation (Delgado-Balbuena et al., 2019). Mean/The mean annual temperature is
112 17.5 \pm 0.5 °C. The topography is characterized by valleys and gentle rolling hills with soils classified as haplic
113 xerosols (associated with lithosols and eutric planosols), and haplic phaeozems (associated with lithosols)
114 (Aguado-Santacruz, 1993). Soils are shallow, with average depth of 0.3-0.4 m containing a cemented layer at
115 \sim 0.5 m deep, with textures dominated by silty clay and sandy loam soils (Aguado-Santacruz, 1993).
116 The study site is a fenced area of \sim 64 ha of semiarid grassland under grazing management. A 6 m high tower
117 was placed at the center of the area of interest to support carbon-energy flux measurements and meteorological
118 instruments-as well. That location allowed an ever-changing and integrated measurement footprint of 320 m,
119 410 m, 580 m, and 260 m from the tower according to the N, E, S, and W orientations, respectively. The study
120 site is part of the MexFlux network (Vargas et al., 2013).

121 2.2 Meteorological and soil measurements

122 Meteorological data ~~was~~were collected continuously at a rate of 1 s and averaged at 30 min intervals using a
123 datalogger (CR3000, Campbell Scientific Inc., Logan, Utah). Variables measured included air temperature and
124 relative humidity (HMP45C, Vaisala, Helsinki, Finland) housed into a radiation shield (R.M. Young Company
125 Inc., Traverse City, MI), incident and reflected shortwave and longwave solar radiation (NR01, Hukseflux,
126 Netherlands), and photosynthetic photon flux density (PPFD, PAR lite, Kipp and Zonen, Delft, the
127 Netherlands). Soil variables were measured at a 5 min frequency and averaged at 30 min intervals. These
128 included volumetric soil water content (CS616, Campbell Sci., Logan, UT) positioned horizontally to 2.5 cm
129 and 15 cm deep, average soil temperature of the top 8 cm soil profile, and soil temperature at 5 cm deep (T108
130 temperature probes, Campbell Scientific Inc., Logan, UT). Soil temperature variables were acquired with
131 another datalogger (CR510, Campbell Scientific Inc., Logan, UT). Precipitation was measured with a bucket
132 rain gauge installed 5 m away from the tower (FTS, Victoria, British Columbia, Canada) at 1 m.a.g.l.

133 2.3 Net ecosystem CO₂ exchange measurements

134 An open path eddy covariance system was placed at 3 m high to cover a fetch of 300 m and used to measure
135 NEE over the semiarid grassland. The system consisted of a three-dimensional sonic anemometer (CSAT-3D,
136 Campbell Sci., Logan, UT) for measuring wind velocity on each polar coordinate (u , v , w) and sonic temperature
137 (θ_s) and an open-path infrared gas analyzer (IRGA, Li-7500, LI-COR Inc., Lincoln, NE) to measure CO₂ and
138 water vapor concentrations. Instruments were mounted in a tower at 3 m above the soil surface, oriented
139 towards the prevailing winds. The IRGA sensor was mounted next to—and 10 cm offset from the anemometer
140 transducers, the center of the IRGA optical path was centered with the distance between the vertically oriented
141 sonic transducers and tilted 45° to avoid dust and water accumulation in the IRGA optical path. Digital signal
142 of both sensors was recorded at a sampling rate of 10 Hz in a datalogger (CR3000, Campbell Scientific Inc.,
143 Logan, UT) (Ocheltree and Loescher 2007). NEE was estimated as:

144 $NEE = \overline{w'CO_2'}$ (1)

145 overbar denotes time averaging (30 min), and primes are the deviations of instantaneous values (at 10 Hz) ~~from~~
 146 ~~a block-averaged mean (30 min)~~ of vertical windspeed (w , $m\ s^{-1}$) and molar volume of CO₂ (CO_2' , μmol
 147 $CO_2\ m^{-3}$), ~~respectively from the block-averaged mean~~. Micrometeorological convention was used, where
 148 negative NEE values stand for ecosystem C uptake (Loescher et al., 2006). We did not estimate a storage flux
 149 because of the low vegetation stature and well-mixed conditions; therefore, we assumed it would be 0 over a
 150 24-h period (Loescher et al., 2006).

151 **2.4 Data processing**

152 Raw eddy covariance data were processed in EdiRe (v1.5.0.10, University of Edinburgh, Edinburgh UK). Wind
 153 velocities, sonic temperature, [CO₂], and [H₂O] signals were despiked, ~~considering outliers (Vickers and Mahrt,~~
 154 ~~1997), any value larger than six standard deviations into a moving window (5 min) was considered a spike,~~
 155 ~~whereas~~ those values with a deviation larger than ~~±8~~ eight standard deviations ~~were flagged as outliers~~. A 2-D
 156 coordinate rotation was applied to sonic anemometer wind velocities to obtain turbulence statistics
 157 perpendicular to the local streamline. Lags between horizontal wind velocity and scalars were removed with a
 158 cross-correlation procedure to maximize the covariance among signals. Carbon and water vapor fluxes were
 159 estimated as molar fluxes ($mol\ m^{-2}\ s^{-1}$) at 30 min block averages, and then they were corrected for air density
 160 fluctuations (WPL correction, Webb et al. 1980). Frequency response correction was done after Massman
 161 (2000). Sensible heat flux was estimated from the covariance between fluctuations of horizontal wind velocity
 162 (w') and sonic temperature (θ'_s). This buoyancy flux was corrected for humidity effects (Schotanus et al. 1983,
 163 Foken et al., 2012).

164 Fluxes were submitted to quality control procedures, i) stationarity (<50%), ii) integral turbulence
 165 characteristics (<50%), iii) flags of IRGA and sonic anemometer (AGC value < 75, Max CSAT diagnostic flag
 166 = 63) which are ~~strongly related with advices of problem measurement due to rain events frequently caused by~~
 167 ~~raindrops on the anemometer transducers and IRGA path~~, iv) screening of flux values into ~~a logical expected~~
 168 magnitudes ($\pm 20\ \mu mol\ CO_2\ m^{-2}\ s^{-1}$), and v) ~~the~~ u* threshold ~~u* = 0.1 m s⁻¹~~ was used to filter nighttime NEE
 169 under poorly developed turbulence. This threshold was defined through the 99% threshold criterion after
 170 Reichstein et al. ~~(2005)~~; (2005); it varied seasonally among years around 0.1 m s⁻¹.

171 Temporally integrated estimates are noted throughout this paper. Because ~~of~~ GEE cannot be measured directly,
 172 it was estimated ~~by ER withdrawal from NEE. The ER was estimated in two ways, 1) it was estimated from~~
 173 ~~light-response curves (see below), and 2) it~~ whereas ER was determined from i) light-response curves and ii)
 174 nighttime NEE data (under PPFD < 10 $\mu mol\ m^{-2}\ s^{-1}$ light conditions). Different ER estimation
 175 ~~method~~ Henceforth, ecosystem respiration derived from light-response curves is indicated throughout the
 176 ~~paper~~ denoted as “ER”, and as “nighttime NEE” when derived from nighttime net ecosystem exchange data.

177 For identifying changes induced by PPT events on GEE and ER, daytime and nighttime NEE data on a one day-
 178 window was adjusted with a rectangular hyperbolic response function to photosynthetic photon flux density
 179 (PPFD; Ruimy et al. 1995).

$$NEE = \frac{\alpha * PPF D * A_{max}}{\alpha * PPF D + A_{max}} + \frac{\alpha * PPF D * \beta}{\alpha * PPF D + \beta} + ER \quad (2)$$

where, α is the apparent quantum yield ($\mu\text{mol CO}_2 \text{ m}^{-2} \text{ s}^{-1} / \mu\text{mol CO}_2 \text{ m}^{-2} \text{ s}^{-1}$), A_{max} is maximum photosynthetic capacity ($\mu\text{mol CO}_2 \text{ m}^{-2} \text{ s}^{-1}$), and ER is the ecosystem respiration ($\mu\text{mol CO}_2 \text{ m}^{-2} \text{ s}^{-1}$). Due to A_{max} is being calculated to unrealistic “infinite” $PPFD$, we calculated a more realistic maximum photosynthetic capacity (A_{2500}), which is maximum photosynthesis at $2500 \mu\text{mol m}^{-2} \text{ s}^{-1}$. Changes and transitions from ER -dominated NEE fluxes to C -gain processes (GEE) were verified with the shape of the light response curve.

We choose this method instead of standard partitioning procedures (i.e. Reichstein et al., 2005 or Lasslop et al., 2010) because we were interested in detecting changes at one day scale. Both algorithms use data windows larger than one day to estimate some parameters and tend to smooth fast changes in soil respiration like the observed in this study. For visually checking for changes in GEE and ER at diel time step, half-hours of NEE were partitioned by Eq. 2 and then averaged by day.

2.5 Gap-filling procedures and characterization of PPT events

Data gaps shorter than two hours were linearly interpolated, whereas gaps larger than two hours were left as empty data. Only daytime- NEE data were used for most of the analysis because of nighttime NEE is subjected to quality problems, ~~which include poor like poorly developed turbulences caused turbulence. Moreover, if mean NEE is estimated from only a few 30-min periods with available data and showed strong divergence from NEE averages if minute nighttime NEE half-hours, the whole estimate may be biased if the full night cycle is not similarly represented among similarly across days. Daily mean ER derived from nighttime NEE data were used for analysis when more than 50% of the data was available after QA/QC procedures.~~ The NEE -related PPT events were selected for analysis based on data quality and availability to evenly cover the daytime cycle (on average more than 85% of NEE data) and then averaged through the day. The daytime-scale was selected to avoid confounding diurnal NEE variability and to achieve robust analyses. All precipitation events between 2011 and 2016 were isolated and then filtered by the number of half-hours accounted for mean daily fluxes.

Mean ER derived from nighttime NEE data were used for analysis only when more than 50% of the data was available after QA/QC procedures. This data was exclusively used for correlation with environmental and soil data (see statistical analysis section). In contrast, daytime NEE (without partitioning) was used for the analysis of changes in NEE fluxes induced by PPT events.

The C flux one day before the PPT event was taken as the reference C flux. ~~Event~~The event-response effect (“priming NEE effect”) was measured as the difference between mean daytime NEE post-event and mean daytime NEE pre-event, such that described as:

$$\Delta NEE = NEE_{\text{post-event}} - NEE_{\text{pre-event}} \quad (3)$$

where, NEE is the daytime NEE average ($\mu\text{mol m}^{-2} \text{ s}^{-1}$).

The same method was used to calculate changes of soil water content at 2.5 and 15 cm depth ($\Delta VWC_{2.5}$ and ΔVWC_{15} , respectively) and change of photosynthetic photon flux density ($\Delta PPF D$)

216) Intervals between PPT events (hereafter inter-event periods, IEP) were counted in days from the last PPT
217 event, regardless of its magnitude.

218 Enhanced vegetation index (EVI) of 250 m spatial resolution and 8-day time-resolution from NASA's MODIS
219 instruments (Didan, 2021) was used ~~as an approximation of to approximate~~ plant leaf activity. The Savitzky-
220 Golay (Yang et al., 2014) filter was used to eliminate outliers of EVI derived from adverse atmospheric
221 conditions.

222 ~~According to the model, where~~ Considering that previous conditions are determinant ~~of for~~ carbon fluxes, data
223 were divided ~~into~~ “fluxes dominated by photosynthesis (carbon uptake)” and “fluxes dominated by ecosystem
224 respiration (carbon efflux)”. A threshold of $-1 \mu\text{mol m}^{-2} \text{s}^{-1}$ of average previous daytime CO_2 flux was used to
225 divide data. This was done to avoid confounding factors, because ~~of the~~ environmental drivers of photosynthesis
226 and respiration may differ in magnitude and direction. Moreover, under photosynthetic conditions is hard to
227 identify if a positive change of NEE (less photosynthesis) was due to an increase of soil respiration or a
228 dampening of photosynthesis by less available radiation under cloudy conditions.

229 To estimate the contribution of the priming effect to the annual carbon balance in the semiarid grassland, we
230 averaged and extrapolated ΔNEE by the number of precipitation events per year. Decaying rates, PPT event
231 size, and previous soil and flux conditions were not considered in this approach. Although this is a rough
232 estimation, it provides a broad overview of how precipitation patterns influence the annual carbon balance. It
233 is important to have this broad overview to better understand the impacts of climate change on carbon cycling
234 in semiarid grasslands.

235 2.6 Statistical analysis

236 Boosted regression trees analysis (BRT; Elith and Leathwick, 2017) were developed to identify the most
237 important variable controlling ~~the this response's~~ priming C effect and thresholds ~~of this response~~. BRT analysis
238 also ~~were was~~ used to identify the form of function, i.e., whether ~~the~~ relationship between independent variables
239 and the priming effect was linear, exponential, sigmoidal, peak from, etc. Independent variables included PPT
240 event size, inter event-periods (IEP), ~~a-priori previous~~, current, and change of volumetric water content (VWC)
241 at two depths (2.5 and 15 cm), soil temperature, previous daytime NEE, enhanced vegetation index (EVI) and
242 change in photosynthetic photon flux density (ΔPPFD). For BRT analysis, data was divided ~~into~~
243 “photosynthesis dominated” and “respiration dominated” data. On the other hand, ~~for to~~ identify delays between
244 C fluxes (ecosystem respiration and gross primary productivity) and precipitation events, a cross-correlation
245 analysis was done. For cross correlation, ~~the~~ parameter of the light response curve was used; the ER was used
246 to identify delays between ecosystem respiration and soil water content at 2.5 cm, and A_{2500} was used to identify
247 delays between gross ecosystem productivity and soil water content at 15 cm, because of ER and A_{2500} were
248 better correlated with soil volumetric water content at 2.5 and 15 cm, respectively. All these variables were
249 detrended before cross-correlation analysis. Finally, linear correlation analyses were performed among
250 environmental variables ~~and~~, priming effect and nighttime ~~NEE (ER)~~, and among independent variables to test
251 for autocorrelations. The “gbm” package (The R core team) was used for performing BRT analysis, whereas

the “astsa” package for R was used to conduct cross-correlation analyses.

3. Results

3.1 Precipitation pattern

Cumulative precipitation for 2011 (288.5 mm) was below the 30-y average for the site (420 mm) and was the worst drought of the last 70-y. In contrast, 2012 received less PPT (393.2 mm), and 2014 and 2016 received more PPT (528.5 and 436 mm, respectively) than average, whereas 2013 (601.6 mm) and 2015 (785.9 mm) were very humid years (Fig. 1). The 6-y differed in precipitation frequency, but they were similar in the size of PPT events with ~60% of the PPT events < 5 mm (Fig. 2a). However, notwithstanding the lower proportion of larger size PPT events (PPT events > 5 mm), they summed similar or even more amount of water than small PPT events (Fig. 2b). Overall, precipitation pattern was characterized by short inter-event periods with 60% of PPT events falling consecutively (IEP < 5 days; Fig. 2c).

Soil saturated after large or recurrent PPT events. Largely, soil moisture was maintained at over a 10% in the wettest years, with the largest peak reaching a 40% in the summer 2014 (Fig. 1b). Most VWC variability was observed at 2.5 cm rather than 15 cm depth, and it was better correlated with precipitation amount per event ($p < 0.05$, $R^2 = 0.72$, Fig. 2d), increasing 0.3 % of VWC per mm of precipitation. The PPT events of 0.25 mm increased the $VWC_{2.5}$ in ~1-2%, but this increase lasted for less than one hour, whereas VWC_{15} increased after PPT ~5 mm (data not shown). Additionally, PPT events and soil moisture dynamics at 15 cm depth were out of phase (up to five days between the PPT event and the SWC_{15} peak, Fig. 2e).

A total of 391 PPT events were isolated over the six years, but 34% did not accomplish with conditions of diel time representativity (>85% of NEE data); thus, 256 events from this 6-y study were used for statistical analysis.

A sample of 100 PPT events was used for the respiration dominated fluxes ($> -1.0 \mu\text{mol m}^{-2} \text{s}^{-1}$) and 156 PPT events for the photosynthesis dominated fluxes ($\leq -1.0 \mu\text{mol m}^{-2} \text{s}^{-1}$). Small precipitation events dominated in our dataset but represented well the precipitation pattern of the site. The sample was integrated by events in the range ranging from 0.25 to 57.1 mm, and a mean of 5.7 ± 0.53 mm (mean \pm 1 SE). Large PPT events occurred after short inter-event periods, and small PPT events were preceded by long inter-event periods. Medium PPT events after long inter-event periods were rare, and extreme large PPT events after long inter-event periods were not observed (Fig. 2f).

The size of the precipitation event (PPT) and previous soil water content at 2.5 cm depth ($\text{pre}VWC_{2.5}$) explained a large variation of change in soil water content at 2.5 cm depth ($\Delta VWC_{2.5}$; $R^2 = 0.54$; Fig. 2d). Best correlation among variables was observed between previous soil water content and soil water content at different depths; for instance, VWC_{15} and $\text{pre}VWC_{15}$ ($R^2 = 0.84$), between the same variables but at 2.5 cm ($R^2 = 0.81$). The change in NEE (priming effect) has did not have a strong relationship with any single variable (Fig. A2).

3.2 Time delays and thresholds

The minimum PPT event that altered NEE rates was 0.25 mm. Overall, the analysis of half-hour fluxes showed almost instantaneous positive response of NEE to the PPT event that exponentially decreased over time into a

287 half to two hours after the PPT event (Fig. A3). ~~The~~ ER rates increased after 0.25 mm PPT events, but we
288 detected a different threshold for GEE where either a larger PPT event or multiple consecutive events (*e.g.*, >
289 40 mm, Fig. 2a) ~~was/were~~ needed, and showed a delay of ~5 days after the positive change in VWC at the 15
290 cm depth, this at the beginning of the growing season (Fig. 3a, b).

291 Cross-correlation analysis of light-response curve parameters showed no lags between ecosystem respiration
292 (ER) and volumetric soil water content at 2.5 cm. (Fig. 3a), whereas there was a lag of 9 days between
293 photosynthetic capacity at 2500 PPFD (A_{2500} ; Fig. 3b) and soil water content, which was larger than the
294 observed at several precipitation ~~evet~~events of 2013 (Fig. 2a, b).

295 The BRT analysis showed sigmoidal relationships between the priming effect and environmental variables with
296 different thresholds. At the respiration-dominated period, a minimum change of soil volumetric water content
297 at 2.5 cm affected positively the carbon flux, but a change larger than 8% in this variable did not induce a larger
298 C efflux (upper threshold; Fig. 4). On the other hand, C priming effect was larger under neutral previous NEE
299 ($preNEE \sim 0$) and decreased in magnitude as $preNEE$ becomes more positive (Fig. 5). Moreover, previous dry
300 conditions at shallow soil depth promoted larger C efflux by the priming effect, and this effect decreased as soil
301 previous conditions were wetter, with a threshold at 15% (Fig. 5). ~~Similar to~~Like the change in soil water
302 content at 2.5 cm, even the lowest PPT event (0.25 mm) caused an increase of C efflux, but with a threshold
303 between 10 - 15 mm. Precipitation events larger than 15 mm did not ~~enhanced~~enhance the priming effect (Fig.
304 5). In contrast, in the photosynthesis dominated period, larger priming effect was observed at more negative
305 $preNEE$ ($-7 \mu\text{mol m}^{-2} \text{s}^{-1}$) and had no more effect at $\sim -4 \mu\text{mol m}^{-2} \text{s}^{-1}$. ~~The priming effect was enhanced by~~
306 ~~dry~~Dry soil conditions ~~enhanced the priming effect~~ at 15 cm depth (< 30%) with a rapid suppression after that.
307 On the other hand, the priming effect was gradually decreasing with reductions ~~of~~in PPFD.

308 Nighttime NEE (ecosystem respiration ~~derived from nighttime NEE data~~) showed correlation with soil water
309 content at the two depths and EVI; however, the relationship was linear at low soil water content, reached a
310 maximum at medium values of VWC, and then decreased with minimum values at high soil water content. The
311 largest ecosystem respiration was observed at ~~higher~~the highest EVI values (Fig. A4)).

312 3.3 Dynamics and drivers of the “Priming effect”

313 The priming effect lasted longer with initial larger ~~change~~changes of NEE, *i.e.*, whereas higher was the priming
314 effect (ΔNEE), the C fluxes lasted more time in returning to initial values (~~previous to~~before the PPT event);
315 however, decreasing NEE rates were better explained by PPT event size than the initial change of NEE (insert
316 Fig. 4). For instance, after a 13.7 mm PPT event and initial daytime $NEE = 5.1 \mu\text{mol m}^{-2} \text{s}^{-1}$, the C flux
317 exponentially decreased at a rate of ~50% of its earlier value, whereas with an initial NEE efflux $\sim 2.5 \mu\text{mol m}^{-2}$
318 s^{-1} , the C flux decreased at a rate of 100% (Fig. 4). Thus, total C efflux was a contribution of the initial change
319 of NEE and the time taken to return to basal values (*i.e.*, decreasing rates).

320 According to BRT analysis, the factor that most influenced the priming effect in the respiration-dominated
321 period was the change of soil water content at 2.5 cm depth ($\Delta VWC_{2.5}$; relative importance, RI = 18%), which
322 was followed by the ~~a-priori~~previous NEE ($preNEE$; RI = 14%), the previous VWC at 2.5 cm depth (RI=14%)

323 and the size of PPT event (RI = 13%). All the other factors had individual RI values lower than 10% (Table 1;
324 Fig. 6). Maximum Δ NEE values were observed at i) larger changes of soil water content at 2.5 cm depth (Fig.
325 6a), ii) previous neutral NEE (i.e., NEE $\sim 0 \mu\text{mol m}^{-2} \text{s}^{-1}$; Fig. 6b), iii) previous dry soil water content at 2.5 cm
326 depth (Fig. 6c), and iv) with large PPT events ($>15 \text{ mm d}^{-1}$; Fig. 6d). The priming NEE effect decreased farther
327 than these limits. In contrast, in the photosynthesis-dominated period, the previous NEE was the most important
328 factor explaining the “priming effect” (RI=33%), ~~whereas 0%.~~ In contrast, the volumetric water content at 15
329 cm depth, the change of photosynthetic photon flux density, and the volumetric water content at 2.5 cm depth
330 followed in importance (Table 1). Larger changes in NEE (priming effect) were observed at i) more negative
331 previous NEE (i.e., under more photosynthetic activity; Fig. 6e), ii) under drier soil water conditions at 15 cm
332 depth (Fig. 6f), iii) with larger changes of PPFD (decrease of PPFD; Fig. 6g), and iv) under air temperature
333 lower than 16 °C and higher than 19 °C (Fig. 6h). There was a large interaction between preVWC_{2.5} and PPT
334 for the respiration-dominated period and between preNEE and ~~APPF~~ΔPPFD for the photosynthesis-dominated
335 period.

336 **3.4 Contribution of priming effect ~~to~~on carbon balance**

337 The carbon balance for ~~this~~these ~~six-year-period~~years for this site was ~~of~~ -126 g C m⁻², with 2955 and -3080 g
338 m⁻² of ecosystem respiration and gross ecosystem exchange, respectively, and varied from a sink of -107 g C
339 m⁻² y⁻¹ to a source of 114 g C m⁻² y⁻¹ (Delgado-Balbuena et al., 2019). Roughly calculation of carbon efflux due
340 to priming effect indicated that extrapolation of mean Δ NEE per event and by year, contributes with 142 g m⁻²
341 for the full six-year period, which corresponds to 5% of total ER flux. In this calculation, parameters like
342 decaying rates, size of PPT event, and previous soil and flux conditions were not considered (modeled) and was
343 subjected to the number of PPT events. Logically, humid years with ~~a greater number of~~more PPT events have
344 more contribution of C efflux by priming effect. Each year contributed with less than 30 g m⁻² y⁻¹.

345 **4. Discussion**

346 **4.1 Dynamics of the “Priming effect”**

347 In agreement with the T-D model, NEE exponentially decreased after the PPT pulse (Fig. 5) to almost the pre-
348 PPT NEE rate. The largest C efflux pulses slowly returned to basal C efflux rates and showed larger NEE
349 remnants than the smaller pulses (Fig. 5). This suggests that more persistent VWC quantities achieved with
350 larger size PPT events promoted larger and longer ~~lasting~~C effluxes~~emissions~~. If the event was large enough
351 to maintain VWC above a threshold for a long time (e.g., above the wilting point for plants) ~~for a long time,~~
352 NEE is expected to remain higher than pre-event rates until nutrients or labile C are depleted (Jarvis et al., 2007;
353 Xu et al., 2004). In contrast, when the PPT event is small, and the soil remains wet for a short-time, the C flux
354 peak will be small and less persistent because of soil dry-out and the activity of microorganisms it is likely to
355 end before soil nutrients are depleted. Thus, ‘priming effect’ decaying rates (-k) likely are more an issue of
356 water availability than nutrient or C source depletion.

357 4.2 Thresholds and time delays of the “Priming carbon flux effect”

358 In our study, the NEE increased immediately (short-time delay) after a PPT event, in accordance with (H1).
359 Moreover, the minimum size of ~~ana~~ PPT event needed to detect NEE change was as low as 0.25 mm d⁻¹, in
360 agreement with (H2). We interpret that immediate daytime PPT-induced responses in NEE and ER rates were
361 dominated by heterotrophic respiration and assume that these microbial communities have evolved to take
362 advantage of this short-term water availability. Short-term responses of < 30-min have also been reported in
363 studies that analyzed soil microorganism activity through molecular and stable isotope techniques (Placella et
364 al., 20012; Unger et al., 2010). Fungi and bacteria on the soil surface have the capability for water-induced re-
365 activation within 1 to 72-h after a PPT event (Placella et al., 2012). Immediate positive NEE increase observed
366 in our study (Fig. A.3) may have resulted from ~~such~~ rapid activation of bacteria displaying highest activity 1-h
367 after wetting. Biological soil ~~erustcrusts~~ (BSC) are assemblages of ~~microorganismmicroorganisms~~ forming
368 crusts on the soil and rock surfaces (Belnap, 2003) common in arid lands. At our site, the BSC covers up to
369 70% of plant interspaces in grazing-excluded conditions and up to 30% in overgrazed sites (Concostrina-Zubiri
370 et al., 2014) with ~~the~~ dominance of ~~actinobaeteriasactinobacteria~~ (e.g., actinomycetes) and
371 ~~eyanobaeteriascyanobacteria~~, which are identified as rapid responders (Bowling et al., 2011). .
372 The maximum priming NEE effect was identified under changes larger than 8% of soil water content at 2.5 cm,
373 previous dry soil, neutral previous NEE, and PPT events > 15 mm. These limits may be defined by several
374 conditions, including; 1) the largest and most intense events did not completely infiltrate into the soil, forming
375 abundant runoff; and moderating the amount of water penetrating the soil profile at ~~a~~ similar depth as that ~~found~~
376 ~~from~~observed for large-size PPT events, 2) oxygen and CO₂ diffusion limitation under high soil VWC
377 dampened soil respiration, 3) all soil aggregates are disrupted at medium soil VWC likely providing no
378 additional nutrient or C substrate at higher VWCs (Bailey et al., 2019; Lado-Monserrat et al., 2014; Homyak et
379 al., 2018; Chen et al., 2019), and 4) a combination of any of these three. ~~Linear~~A linear relationship between
380 PPT event size, preVWC_{2.5} and ΔVWC_{2.5} (Fig. 2d) showed that there was not a ~~strong~~substantial limitation of
381 water infiltration into the soil at shallow depths, discarding in some way the first condition, whereas the
382 reduction of ER rates in nighttime NEE data after VWC_{2.5}> 12%, and daytime ΔNEE reductions under higher
383 preVWC_{2.5} supports the second mechanism (Fig. 6, and A4).

384 4.2 The ER and GEE threshold and time delays difference

385 The smallest PPT events only stimulated ER rates, with no apparent change observed in GEE (Fig. 3). Even a
386 large PPT event of 20 mm d⁻¹ recorded in May 2013 (Fig. 3) did not induce an increase in GEE. In contrast,
387 larger or consecutive PPT events that reached deeper soil profiles stimulated GEE (cumulative PPT > 40mm).
388 These results also explain why the ~~a-priori~~previous soil moisture and the change of ~~VWCsoil moisture~~ (2.5 cm
389 depth) better explained ΔNEE at the respiration-dominated period, rather than soil moisture at 15 cm depth (Fig
390 5); this confirms our notion that soil microorganism activity was the source of the immediate CO₂ efflux. In
391 contrast, VWC at 15 cm depth was the second most important factor explaining ~~the~~ priming NEE effect in the
392 photosynthesis-dominated period. Additionally, the change of PPFD during the photosynthesis-dominated

393 period ~~affected~~ positively affected the priming effect (Fig. 6), ~~it means meaning~~ that ~~reduction of carbon uptake~~
394 ~~by cloudy conditions~~ was larger reduced carbon uptake rather than ~~the stimulus of PPT and stimulated~~ ecosystem
395 respiration ~~by the increase of soil moisture~~.

396 The low PPT threshold that stimulated ER agrees with results from other studies in arid ecosystems (and are
397 even lower). PPT events as small as 3 mm induced respiration of biological soil crusts (Kurc and Small, 2007),
398 and PPT events <10 mm d⁻¹ on a shortgrass steppe promoted net loss of C (Parton et al., 2012). Moreover,
399 Medina-Roldán et al. (2013) at the same study site showed an increase of 36% and 34% of extractable NH₄⁺
400 and NO₃⁻, respectively, after a PPT event of 10 mm, which is an indicative of soil biological activity. However,
401 the dominant species at our site, *B. gracilis*, was reported to respond to PPT events as small as 5 mm (Sala and
402 Lauenroth, 1982), which was the PPT threshold we were expecting. Instead, this study found that large or
403 consecutive PPT events had to occur before an effect on GEE was observed (Fig 3). Nevertheless, ~~it is~~
404 interesting to note we highlight that small PPT events in arid ecosystems that do not lead to C uptake may
405 alleviate stress after severe droughts, rehydrating plant tissues and helping plants to respond faster after larger
406 PPT events (Sala and Lauenroth, 1982; Aguirre-Gutiérrez et al., 2019; Thomey et al 2011).

407 Causes of larger time-delays in GEE than ER ~~is are~~ likely due to the delay between the PPT event and the
408 infiltration of water to a given soil layer (e.g., 15 cm depth; Fig. 2e), and the time spent for regrowing of new
409 roots and leaves (Ogle and Reynolds, 2004). These processes promote C losses rather than C uptake in the early
410 growing season (Huxman et al., 2004; Delgado-Balbuena et al., 2019). In contrast, ER was primarily controlled
411 by soil moisture at shallow soil layers that moist immediately after any PPT event and may activate soil
412 microorganism just a few hours after soil wetting as discussed above.

413 **4.3 Influence of event size and a priori conditions**

414 The magnitude of the priming effect was determined by the size of the PPT event and mainly by the Δ VWC as
415 well as the ~~prior~~previous condition of the ecosystem (i.e., previous C flux, and previous soil VWC). These
416 results agree with (H3) that proposed the PPT event size and previous conditions of the semiarid grassland
417 would control the magnitude of the “priming NEE effect”. The ~~a-priori~~previous VWC offers insight into the
418 potential dry-wet shock experienced by soil aggregates and ~~microorganism~~microorganisms (Haynes and Swift,
419 1990) and thus accounts for nutrient and labile C accumulation in soil (Bailey et al., 2019).

420 Results indicated that larger C effluxes were induced from medium amount of PPT when the previous soil
421 conditions were dry and had ~~a-preceding an initial~~ value of NEE = ~0. Several mechanisms can explain this
422 result: i) the accumulation of nutrients and labile C into the soil (Schimel and Bennet, 2004) because low activity
423 of microorganisms (NEE ~ 0) under dry soil (Homyak et al., 2018), ii) if soil VWC is maintained for ~~a-long an~~
424 extended period above a threshold, then soil microbial activity exhaust labile C sources (Jarvis et al., 2007;
425 Fierer and Schimel, 2002). Consequently, recalcitrant C sources subjected to microbial decomposition decrease
426 mineralization rates (Van Gestel et al., 1993).

4.4 Importance of the priming effect in the annual C balance.

~~We expected~~Our results do not support the hypothesis that a significant contribution of C release from the “priming effect” ~~to decrease~~decreases the net annual C uptake of the semiarid grassland (H4). ~~Contribution~~The contribution of ~~this~~these short-term C efflux events to annual C balances accounted for a considerable amount, but it was a small contribution if it is considered into the ecosystem respiration flux, which was almost 3000 g m⁻² s⁻¹. (Delgado-Balbuena et al., 2019). Notwithstanding its contribution is ~~apparently~~ low (~5% of ecosystem respiration), it is important considering that the annual C balance (NEE) is a small fraction of the difference between ER and GEE, ~~thus~~. Thus, a 5% of C released represents up to 500% of the net C uptake during an almost neutral year and may turn a C sink ecosystem into a net C source. ~~Therefore, we cannot reject H4.~~

4.5 Priming effect and climate change perspectives.

The low $\Delta SWC_{2.5}$ and PPT threshold for respiration suggests that almost all PPT events occurring in the semiarid grasslands will produce C efflux but will be limited by the characteristics of the PPT pattern and previous soil conditions at the site. Therefore, we expect that small PPT events with ~~dry~~previous dry conditions or long inter-event periods will limit the priming effect by maintaining the system below threshold conditions. Moreover, consecutive PPT events or large PPT events should keep soil water content above a threshold that will promote C uptake by photosynthesis, which in the long term will overcome C ~~loses~~loss from the priming effect. However, climate change scenarios forecast for the semiarid grassland in Mexico a decrease ~~of~~in winter PPT and the increase ~~of~~in storms with larger inter-event periods, which are conditions for increasing the amount of C released by the priming effect (Arca et al., 2021; Darenova et al., 2019).

~~It is necessary a further~~Further analysis of the effect of these PPT events on vegetation is necessary since productivity will also depend on PPT event size and will be modulated by previous soil conditions. Additionally, it is likely that productivity will benefit more ~~of~~from accumulated PPT than respiration. Still, more analysis of projected PPT scenarios is required to ~~forecast~~accurately forecast the ~~PPT pattern~~contribution of the Birch effect to C balance under more frequent droughts, ~~and to know if the current PPT pattern of dry-wet years will prevail.~~ In this sense, parameterizing a model like ~~de~~the T-D model will provide valuable information ~~of~~on more accurate C effluxes from the priming effect and how it will be affected by changes ~~of~~in precipitation pattern. Only after that, will we ~~will~~ be able to predict the course of the semiarid grassland as a source or sink of C under PPT pattern changes.

5. Conclusions

Previous soil water conditions and previous NEE were the most important factors controlling the priming effect in the semiarid grassland. The ~~size of~~precipitation size had an important role in explaining the priming effect but only in the respiration-dominated period. Delays between change responses ~~of change~~ at deeper soil layer and for regrowing processes could hide the relationship between precipitation and priming effect during the photosynthesis-dominated period. ~~Importance~~The importance of the priming effect in the carbon balance could

461 be more ~~important~~relevant under forecasted changes in precipitation ~~pattern~~patterns by increasing in both the
462 frequency and intensity the dry-wet soil cycles. ~~A further~~Further analysis of the effect of this change of
463 precipitation ~~pattern~~pattern on ecosystem productivity is necessary before we can conclude about changes in the
464 carbon balance of the semiarid grassland.

465
466 *Author contributions.* The study was conceived by JD, TA, HL, and RV. JD, TA and CAA get and processed
467 eddy covariance data. JD, TAR, and LFM implemented the method and performed the data analyses. TAR and
468 CAA get and processed the Enhanced Vegetation Index data. TA, HL, LFM, and RV helped to interpret the
469 results. JD, TA, HL, and RV prepared the first draft, and all authors contributed to discussion of results and the
470 revisions of the paper.

471
472 *Competing interests.* The authors declare that they have no conflict of interest.

473
474 *Availability of data.* The datasets used ~~and/or analyzed during the current~~for this study are available ~~from~~
475 Zenodo <https://doi.org/10.5281/zenodo.7379206>

476 Acknowledgments

477 ~~Authors~~The authors thank INIFAP for the facilities at CENID Agricultura Familiar research site in Ojuelos,
478 Jalisco, to carry out this study. This research was funded by SEMARNAT-CONACYT, project reference
479 number 108000, CB 2008-01 102855, CB 2013 220788 given to TA, and CONACYT CF 320641 given to JDB.
480 HWL acknowledges the National Science Foundation (NSF) for on-going support under the cooperative support
481 agreement (EF-1029808) to Battelle. Any opinions, findings, and conclusions, or recommendations expressed
482 in this material are those of the authors and do not necessarily reflect the views of our sponsoring agencies.

483 References

- 484 [Aguado-Santacruz, G. A.: Efecto de factores ambientales sobre la dinámica vegetacional en pastizales de los](#)
485 [Llanos de Ojuelos, Jalisco: un enfoque multivariable, Colegio de Postgraduados, Chapingo, México, 155 pp.,](#)
486 [1993.](#)
487 [Aguirre-Gutiérrez, C. A., Holwerda, F., Goldsmith, G. R., Delgado, J., Yopez, E., Carbajal, N., Escoto-](#)
488 [Rodríguez, M., and Arredondo, J. T.: The importance of dew in the water balance of a continental semiarid](#)
489 [grassland, J. Arid Environ., 168, 26–35, <https://doi.org/10.1016/j.jaridenv.2019.05.003>, 2019.](#)
490 [Arca, V., Power, S. A., Delgado-Baquerizo, M., Pendall, E., and Ochoa-Hueso, R.: Seasonal effects of altered](#)
491 [precipitation regimes on ecosystem-level CO2 fluxes and their drivers in a grassland from Eastern Australia,](#)
492 [Plant Soil, 460, 435–451, <https://doi.org/10.1007/s11104-020-04811-x>, 2021.](#)
493 [Bailey, V. L., Pries, C. H., and Lajtha, K.: What do we know about soil carbon destabilization?, Environ. Res.](#)
494 [Lett., 14, <https://doi.org/10.1088/1748-9326/ab2c11>, 2019.](#)

495 [Bastida, F., García, C., Fierer, N., Eldridge, D. J., Bowker, M. A., Abades, S., Alfaro, F. D., Asefaw Berhe, A.,](#)
496 [Cutler, N. A., Gallardo, A., García-Velázquez, L., Hart, S. C., Hayes, P. E., Hernández, T., Hseu, Z. Y.,](#)
497 [Jehmlich, N., Kirchmair, M., Lambers, H., Neuhauser, S., Peña-Ramírez, V. M., Pérez, C. A., Reed, S. C.,](#)
498 [Santos, F., Siebe, C., Sullivan, B. W., Trivedi, P., Vera, A., Williams, M. A., Luis Moreno, J., and Delgado-](#)
499 [Baquerizo, M.: Global ecological predictors of the soil priming effect, *Nat. Commun.*, 10, 1–9,](#)
500 <https://doi.org/10.1038/s41467-019-11472-7>, 2019.

501 [Belnap, J.: Microbes and microfauna associated with biological soil crusts, *Biol. Soil Crusts Struct. Funct.*](#)
502 [Manag.](#), 167–174, 2003.

503 [Birch, H. F.: Mineralisation of plant nitrogen following alternate wet and dry conditions, 1964.](#)

504 [Borken, W. and Matzner, E.: Reappraisal of drying and wetting effects on C and N mineralization and fluxes](#)
505 [in soils, *Glob. Chang. Biol.*, 15, 808–824, https://doi.org/10.1111/j.1365-2486.2008.01681.x](#), 2009.

506 [Bowling, D. R., Grote, E. E., and Belnap, J.: Rain pulse response of soil CO₂ exchange by biological soil crusts](#)
507 [and grasslands of the semiarid Colorado Plateau, United States, *J. Geophys. Res. Biogeosciences*,](#)
508 <https://doi.org/10.1029/2011JG001643>, 2011.

509 [Burrell, A. L., Evans, J. P., and De Kauwe, M. G.: Anthropogenic climate change has driven over 5 million](#)
510 [km² of drylands towards desertification, *Nat Commun.*, 11, 3853, https://doi.org/10.1038/s41467-020-17710-7,](#)
511 [2020.](#)

512 [Christensen, J. H., Hewitson, B., Busuioc, A., Chen, A., Gao, X., Held, I., Jones, R., Kolli, R. K., Kwon, W.](#)
513 [T., Laprise, R., Magana Rueda, V., Mearns, L., Menéndez, C. G., Räisänen, J., Rinke, A., Sarr, A., and Whetton,](#)
514 [P.: Regional Climate Projections, in: *Climate Change 2007: The Physical Science Basis. Contribution of*](#)
515 [Working Group I to the Fourth Assessment Report of the Intergovernmental Panel on Climate Change](#), edited
516 [by: Solomon, S., Qin, D., Manning, M., Chen, Z., Marquis, M., Averyt, K. B., Tignor, M., and Miller, H. L.,](#)
517 [Cambridge University Press, Cambridge, United Kingdom and New York, NY, USA, 847–940,](#)
518 <https://doi.org/10.1080/07341510601092191>, 2007.

519 [Chen, L., Liu, L., Qin, S., Yang, G., Fang, K., Zhu, B., Kuzyakov, Y., Chen, P., Xu, Y., and Yang, Y.:](#)
520 [Regulation of priming effect by soil organic matter stability over a broad geographic scale, *Nat. Commun.*, 10,](#)
521 [1–10, https://doi.org/10.1038/s41467-019-13119-z](#), 2019.

522 [Collins, S. L., Sinsabaugh, R. L., Crenshaw, C., Green, L., Porrás-Alfaro, A., Stursova, M., and Zeglin, L. H.:](#)
523 [Pulse dynamics and microbial processes in aridland ecosystems: Pulse dynamics in aridland soils, *J. Ecol.*, 96,](#)
524 [413–420, https://doi.org/10.1111/j.1365-2745.2008.01362.x](#), 2008.

525 [Concostrina-Zubiri, L., Huber-Sannwald, E., Martínez, I., Flores Flores, J. L., Reyes-Agüero, J. A., Escudero,](#)
526 [A., and Belnap, J.: Biological soil crusts across disturbance-recovery scenarios: Effect of grazing regime on](#)
527 [community dynamics, *Ecol. Appl.*, 24, 1863–1877, https://doi.org/10.1890/13-1416.1](#), 2014.

528 [Darenova, E., Holub, P., Krupkova, L., and Pavelka, M.: Effect of repeated spring drought and summer heavy](#)
529 [rain on managed grassland biomass production and CO₂ efflux, *J. Plant Ecol.*, 10, 476–485,](#)
530 <https://doi.org/10.1093/jpe/rtw058>, 2017.

531 [Delgado-Balbuena, J., Arredondo, J. T., Loescher, H. W., Pineda-Martínez, L. F., Carbajal, J. N., and Vargas,](#)
532 [R.: Seasonal Precipitation Legacy Effects Determine the Carbon Balance of a Semiarid Grassland, *J. Geophys.*](#)

533 [Res. Biogeosciences, 124, 987–1000, https://doi.org/10.1029/2018JG004799, 2019.](https://doi.org/10.1029/2018JG004799)

534 [Didan, K. MOD13Q1 MODIS/Terra Vegetation Indices 16-Day L3 Global 250m SIN Grid V061. NASA](https://doi.org/10.5067/MODIS/MOD13Q1.061)

535 [EOSDIS Land Processes DAAC. https://doi.org/10.5067/MODIS/MOD13Q1.061, 2021.](https://doi.org/10.5067/MODIS/MOD13Q1.061)

536 [Easterling, D. R., Meehl, G. A., Parmesan, C., Changnon, S. A., Karl, T. R., and Mearns, L. O.: Climate](https://doi.org/10.1126/science.1201531)

537 [Extremes: Observations, Modeling, and Impacts, *Science* \(80-. \), 289, 2068–2074, 2000.](https://doi.org/10.1126/science.1201531)

538 [Elith, J. and Leathwick, J.: Boosted regression trees for ecological modelling and prediction, *R Doc.*, 1–22,](https://doi.org/10.1111/1365-3113.12522)

539 [2017.](https://doi.org/10.1111/1365-3113.12522)

540 [Fierer, N. and Schimel, J. P.: Effects of drying–rewetting frequency on soil carbon and nitrogen transformations,](https://doi.org/10.1016/S0038-0717(02)00007-X)

541 [Soil Biol. Biochem., 34, 777–787, https://doi.org/10.1016/S0038-0717\(02\)00007-X, 2002.](https://doi.org/10.1016/S0038-0717(02)00007-X)

542 [Foken, T., Leuning, R., Oncley, S. R., Mauder, M., and Aubinet, M.: Corrections and Data Quality Control, in:](https://doi.org/10.1007/978-94-007-2351-1_4)

543 [Eddy Covariance, Springer Netherlands, Dordrecht, 85–131, https://doi.org/10.1007/978-94-007-2351-1_4,](https://doi.org/10.1007/978-94-007-2351-1_4)

544 [2012.](https://doi.org/10.1007/978-94-007-2351-1_4)

545 [Van Gestel, M., Merckx, R., and Vlassak, K.: Microbial biomass and activity in soils with fluctuating water](https://doi.org/10.1016/0016-7061(93)90140-G)

546 [contents, *Geoderma*, 56, 617–626, https://doi.org/10.1016/0016-7061\(93\)90140-G, 1993.](https://doi.org/10.1016/0016-7061(93)90140-G)

547 [Haynes, R. J. and Swift, R. S.: Stability of soil aggregates in relation to organic constituents and soil water](https://doi.org/10.1111/j.1365-2389.1990.tb00046.x)

548 [content, *J. Soil Sci.*, 41, 73–83, https://doi.org/10.1111/j.1365-2389.1990.tb00046.x, 1990.](https://doi.org/10.1111/j.1365-2389.1990.tb00046.x)

549 [Homyak, P. M., Blankinship, J. C., Slessarev, E. W., Schaeffer, S. M., Manzoni, S., and Schimel, J. P.: Effects](https://doi.org/10.1002/ecy.2473)

550 [of altered dry season length and plant inputs on soluble soil carbon, *Ecology*, 99, 2348–2362,](https://doi.org/10.1002/ecy.2473)

551 [https://doi.org/10.1002/ecy.2473, 2018.](https://doi.org/10.1002/ecy.2473)

552 [Huxman, T. E., Smith, M. D., Fay, P. A., Knapp, A. K., Shaw, M. R., Loik, M. E., Smith, S. D., Tissue, D. T.,](https://doi.org/10.1038/nature02561)

553 [Zak, J. C., Weltzin, J. F., Pockman, W. T., Sala, O. E., Haddad, B. M., Harte, J., Koch, G. W., Schwinning, S.,](https://doi.org/10.1038/nature02561)

554 [Small, E. E., and Williams, D. G.: Convergence across biomes to a common rain-use efficiency, *Nature*, 429,](https://doi.org/10.1038/nature02561)

555 [651–654, https://doi.org/10.1038/nature02561, 2004a.](https://doi.org/10.1038/nature02561)

556 [Huxman, T. E., Snyder, K. A., Tissue, D., Leffler, A. J., Ogle, K., Pockman, W. T., Sandquist, D. R., Potts, D.](https://doi.org/10.1007/s00442-004-1682-4)

557 [L., and Schwinning, S.: Precipitation pulses and carbon fluxes in semiarid and arid ecosystems, *Oecologia*, 141,](https://doi.org/10.1007/s00442-004-1682-4)

558 [254–268, https://doi.org/10.1007/s00442-004-1682-4, 2004b.](https://doi.org/10.1007/s00442-004-1682-4)

559 [Jarvis, P., Rey, A., Petsikos, C., Wingate, L., Rayment, M., Pereira, J., Banza, J., David, J., Miglietta, F.,](https://doi.org/10.1007/s11099-007-9100-1)

560 [Borghetti, M., Manca, G., and Valentini, R.: Drying and wetting of Mediterranean soils stimulates](https://doi.org/10.1007/s11099-007-9100-1)

561 [decomposition and carbon dioxide emission: the “Birch effect,” *Tree Physiol.*, 27, 929–940, 2007.](https://doi.org/10.1007/s11099-007-9100-1)

562 [Kim, D.-G., Vargas, R., Bond-Lamberty, B., and Turetsky, M. R.: Effects of soil rewetting and thawing on soil](https://doi.org/10.1016/j.biogeosciences.2012.05.012)

563 [gas fluxes: a review of current literature and suggestions for future research, *Biogeosciences*, 9, 2459–2483,](https://doi.org/10.1016/j.biogeosciences.2012.05.012)

564 [https://doi.org/10.5194/bg-9-2459-2012, 2012.](https://doi.org/10.5194/bg-9-2459-2012)

565 [Knapp, A. K., Hoover, D. L., Wilcox, K. R., Avolio, M. L., Koerner, S. E., La Pierre, K. J., Loik, M. E., Luo,](https://doi.org/10.1111/gcb.12888)

566 [Y., Sala, O. E., and Smith, M. D.: Characterizing differences in precipitation regimes of extreme wet and dry](https://doi.org/10.1111/gcb.12888)

567 [years: Implications for climate change experiments, *Glob. Chang. Biol.*, 21, 2624–2633,](https://doi.org/10.1111/gcb.12888)

568 [https://doi.org/10.1111/gcb.12888, 2015.](https://doi.org/10.1111/gcb.12888)

569 [Korell, L., Auge, H., Chase, J. M., Harpole, W. S., and Knight, T. M.: Responses of plant diversity to](https://doi.org/10.1111/1365-3113.12522)

570 [precipitation change are strongest at local spatial scales and in drylands, *Nat Commun*, 12, 2489,](https://doi.org/10.1111/1365-3113.12522)

571 <https://doi.org/10.1038/s41467-021-22766-0>, 2021.

572 [Kurc, S. A. and Small, E. E.: Dynamics of evapotranspiration in semiarid grassland and shrubland ecosystems](#)

573 [during the summer monsoon season, central New Mexico, *Water Resour. Res.*, 40, W09305, 2004.](#)

574 [Lado-Monserrat, L., Lull, C., Bautista, I., Lidon, A., and Herrera, R.: Soil moisture increment as a controlling](#)

575 [variable of the “Birch effect”. Interactions with the pre-wetting soil moisture and litter addition, *Plant Soil*, 379,](#)

576 [21–34, <https://doi.org/10.1007/s11104-014-2037-5>, 2014.](#)

577 [Lal, R.: Carbon Sequestration in Dryland Ecosystems, *Environ. Manage.*, 33, 528–544,](#)

578 [https://doi.org/10.1007/s00267-003-9110-9, 2004.](#)

579 [Lauenroth, W. K. and Sala, O. E.: Long-term forage production of North American shortgrass steppe,](#)

580 [https://doi.org/10.2307/1941874, 1992.](#)

581 [Loescher, H. W., Law, B. E., Mahrt, L., Hollinger, D. Y., Campbell, J., and Wofsy, S. C.: Uncertainties in, and](#)

582 [interpretation of, carbon flux estimates using eddy covariance techniques, *J. Geophys. Res.*, 111, 19,](#)

583 [https://doi.org/10.1029/2005JD006932, 2006.](#)

584 [Loik, M. E., Breshears, D. D., Lauenroth, W. K., and Belnap, J.: A multi-scale perspective of water pulses in](#)

585 [dryland ecosystems: Climatology and ecohydrology of the western USA, *Oecologia*, 141, 269–281,](#)

586 [https://doi.org/10.1007/s00442-004-1570-y, 2004.](#)

587 [Maliva, R. and Missimer, T.: *Microgravity*, Springer Berlin Heidelberg, 329–342, 2012.](#)

588 [Massman, W. J.: A simple method for estimating frequency response corrections for eddy covariance systems,](#)

589 [Agric. For. Meteorol., 104, 185–198, \[https://doi.org/10.1016/S0168-1923\\(00\\)00164-7\]\(https://doi.org/10.1016/S0168-1923\(00\)00164-7\), 2000.](#)

590 [Medina-Roldán, E., Arredondo Moreno, J. T., García Moya, E., and Huerta Martínez, F. M.: Soil Water Content](#)

591 [Dynamics Along a Range Condition Gradient in a Shortgrass Steppe, *Rangel. Ecol. Manag.*, 60, 79–87,](#)

592 [https://doi.org/10.2111/05-219R2.1, 2007.](#)

593 [Nielsen, U. N. and Ball, B. A.: Impacts of altered precipitation regimes on soil communities and](#)

594 [biogeochemistry in arid and semi-arid ecosystems, *Glob Change Biol*, 21, 1407–1421,](#)

595 [https://doi.org/10.1111/gcb.12789, 2015.](#)

596 [Noy-Meir, I.: Desert Ecosystems: Environment and Producers, *Annu. Rev. Ecol. Syst.*, 4, 25–51, 1973.](#)

597 [Ocheltree, T. W. and Loescher, H. W.: Design of the AmeriFlux portable eddy covariance system and](#)

598 [uncertainty analysis of carbon measurements, *J. Atmos. Ocean. Technol.*, 24, 1389–1406,](#)

599 [https://doi.org/10.1175/JTECH2064.1, 2007.](#)

600 [Ogle, K. and Reynolds, J. F.: Plant responses to precipitation in desert ecosystems: integrating functional types,](#)

601 [pulses, thresholds, and delays, *Oecologia*, 141, 282–294, <https://doi.org/10.1007/s00442-004-1507-5>, 2004.](#)

602 [Parton, W., Morgan, J., Smith, D., Del Grosso, S., Prihodko, L., LeCain, D., Kelly, R., and Lutz, S.: Impact of](#)

603 [precipitation dynamics on net ecosystem productivity, *Glob. Chang. Biol.*, 18, 915–927,](#)

604 [https://doi.org/10.1111/j.1365-2486.2011.02611.x, 2012.](#)

605 [Placella, S. A., Brodie, E. L., and Firestone, M. K.: Rainfall-induced carbon dioxide pulses result from](#)

606 [sequential resuscitation of phylogenetically clustered microbial groups, *Proc. Natl. Acad. Sci.*, 109, 10931–](#)

607 [10936, <https://doi.org/10.1073/pnas.1204306109>, 2012.](#)

608 [Reichmann, L. G., Sala, O. E., and Peters, D. P. C.: Water controls on nitrogen transformations and stocks in](#)

609 [an arid ecosystem, *Ecosphere*, 4, 1–17, https://doi.org/10.1890/ES12-00263.1, 2013.](https://doi.org/10.1890/ES12-00263.1)

610 [Reichstein, M., Falge, E., Baldocchi, D., Papale, D., Aubinet, M., Berbigier, P., Bernhofer, C., Buchmann, N.,](https://doi.org/10.1111/j.1365-2486.2005.001002.x)

611 [Gilmanov, T., Granier, A., Grünwald, T., Havránková, K., Ilvesniemi, H., Janous, D., Knohl, A., Laurila, T.,](https://doi.org/10.1111/j.1365-2486.2005.001002.x)

612 [Lohila, A., Loustau, D., Matteucci, G., Meyers, T., Miglietta, F., Ourcival, J. M., Pumpanen, J., Rambal, S.,](https://doi.org/10.1111/j.1365-2486.2005.001002.x)

613 [Rotenberg, E., Sanz, M., Tenhunen, J., Seufert, G., Vaccari, F., Vesala, T., Yakir, D., and Valentini, R.: On the](https://doi.org/10.1111/j.1365-2486.2005.001002.x)

614 [separation of net ecosystem exchange into assimilation and ecosystem respiration: Review and improved](https://doi.org/10.1111/j.1365-2486.2005.001002.x)

615 [algorithm, https://doi.org/10.1111/j.1365-2486.2005.001002.x, 2005.](https://doi.org/10.1111/j.1365-2486.2005.001002.x)

616 [Ruimy, A., Jarvis, P. G., Baldocchi, D. D., Saugier, B., and M. Begon and A.H. Fitter: CO₂ Fluxes over Plant](https://doi.org/10.1002/9781118164332.ch1)

617 [Canopies and Solar Radiation: A Review, vol. Volume 26, Academic Press, 1–68, 1995.](https://doi.org/10.1002/9781118164332.ch1)

618 [Sala, O. E. and Lauenroth, W. K.: Small rainfall events: An ecological role in semiarid regions, *Oecologia*, 53,](https://doi.org/10.1007/BF00389004)

619 [301–304, https://doi.org/10.1007/BF00389004, 1982.](https://doi.org/10.1007/BF00389004)

620 [Schotanus, P., Nieuwstadt, F. T. M., and De Bruin, H. A. R.: Temperature measurement with a sonic](https://doi.org/10.1007/BF00164332)

621 [anemometer and its application to heat and moisture fluxes, *Boundary-Layer Meteorol.*, 26, 81–93,](https://doi.org/10.1007/BF00164332)

622 [https://doi.org/10.1007/BF00164332, 1983.](https://doi.org/10.1007/BF00164332)

623 [Thomey, M. L., Collins, S. L., Vargas, R., Johnson, J. E., Brown, R. F., Natvig, D. O., and Friggens, M. T.:](https://doi.org/10.1111/j.1365-2486.2010.02363.x)

624 [Effect of precipitation variability on net primary production and soil respiration in a Chihuahuan Desert](https://doi.org/10.1111/j.1365-2486.2010.02363.x)

625 [grassland: Precipitation variability in desert grasslands, *Global Change Biology*, 17, 1505–1515,](https://doi.org/10.1111/j.1365-2486.2010.02363.x)

626 [https://doi.org/10.1111/j.1365-2486.2010.02363.x, 2011.](https://doi.org/10.1111/j.1365-2486.2010.02363.x)

627 [Turner, B. and Haygarth, P. M.: Phosphorus](https://doi.org/10.1002/(SICI)1097-0177(199909)216:1<1::AID-DVDY1>3.0.CO;2-T)

628 [solubilization in rewetted soils, *Nature*, 411, 258, https://doi.org/10.1002/\(SICI\)1097-](https://doi.org/10.1002/(SICI)1097-0177(199909)216:1<1::AID-DVDY1>3.0.CO;2-T)

629 [0177\(199909\)216:1<1::AID-DVDY1>3.0.CO;2-T, 2001.](https://doi.org/10.1002/(SICI)1097-0177(199909)216:1<1::AID-DVDY1>3.0.CO;2-T)

630 [Vargas, R., Sánchez-Cañete P., E., Serrano-Ortiz, P., Curiel Yuste, J., Domingo, F., López-Ballesteros, A., and](https://doi.org/10.3390/soilsystems2030047)

631 [Oyonarte, C.: Hot-Moments of Soil CO₂ Efflux in a Water-Limited Grassland, *Soil Syst.*, 2, 47,](https://doi.org/10.3390/soilsystems2030047)

632 [https://doi.org/10.3390/soilsystems2030047, 2018.](https://doi.org/10.3390/soilsystems2030047)

633 [Vargas, R., Collins, S. L., Thomey, M. L., Johnson, J. E., Brown, R. F., Natvig, D. O., and Friggens, M. T.:](https://doi.org/10.1111/j.1365-2486.2011.02628.x)

634 [Precipitation variability and fire influence the temporal dynamics of soil CO₂ efflux in an arid grassland, *Global*](https://doi.org/10.1111/j.1365-2486.2011.02628.x)

635 [Change Biology, 18, 1401–1411, https://doi.org/10.1111/j.1365-2486.2011.02628.x, 2012.](https://doi.org/10.1111/j.1365-2486.2011.02628.x)

636 [Vargas, R., Yépez, E. A., Andrade, J. L., Ángeles, G., Arredondo, T., Castellanos, A. E., Delgado-Balbuena,](https://doi.org/10.1016/S0187-6236(13)71079-8)

637 [J., Garatuzza-Payán, J., González Del Castillo, E., Oechel, W., Rodríguez, J. C., Sánchez-Azofeifa, A., Velasco,](https://doi.org/10.1016/S0187-6236(13)71079-8)

638 [E., Vivoni, E. R., and Watts, C.: Progress and opportunities for monitoring greenhouse gases fluxes in Mexican](https://doi.org/10.1016/S0187-6236(13)71079-8)

639 [ecosystems: the MexFlux network, *Atmósfera*, 26, 325–336, https://doi.org/10.1016/S0187-6236\(13\)71079-8,](https://doi.org/10.1016/S0187-6236(13)71079-8)

640 [2013.](https://doi.org/10.1016/S0187-6236(13)71079-8)

641 [Wang, B., Chen, Y., Li, Y., Zhang, H., Yue, K., Wang, X., Ma, Y., Chen, J., Sun, M., Chen, Z., and Wu, Q.:](https://doi.org/10.1111/gcb.15875)

642 [Differential effects of altered precipitation regimes on soil carbon cycles in arid versus humid terrestrial](https://doi.org/10.1111/gcb.15875)

643 [ecosystems, *Global Change Biology*, 27, 6348–6362, https://doi.org/10.1111/gcb.15875, 2021.](https://doi.org/10.1111/gcb.15875)

644 [Webb, E. K., Pearman, G. I., and Leuning, R.: Correction of flux measurements for density effects due to heat](https://doi.org/10.1002/qj.49710644707)

645 [and water vapour transfer, https://doi.org/10.1002/qj.49710644707, January 1980.](https://doi.org/10.1002/qj.49710644707)

646 [Xu, L., Baldocchi, D. D., and Tang, J.: How soil moisture, rain pulses, and growth alter the response of](https://doi.org/10.1111/gbc.12111)

ecosystem respiration to temperature, *Global Biogeochem. Cycles*, 18, n/a-n/a,

647 <https://doi.org/10.1029/2004GB002281>, 2004.
648 [Yang, X., Tang, J., and Mustard, J. F.: Beyond leaf color: Comparing camera-based phenological metrics with](#)
649 [leaf biochemical, biophysical, and spectral properties throughout the growing season of a temperate deciduous](#)
650 [forest, J. Geophys. Res. Biogeosciences, 119, 181–191, https://doi.org/10.1002/2013JG002460, 2014.](#)
651
652

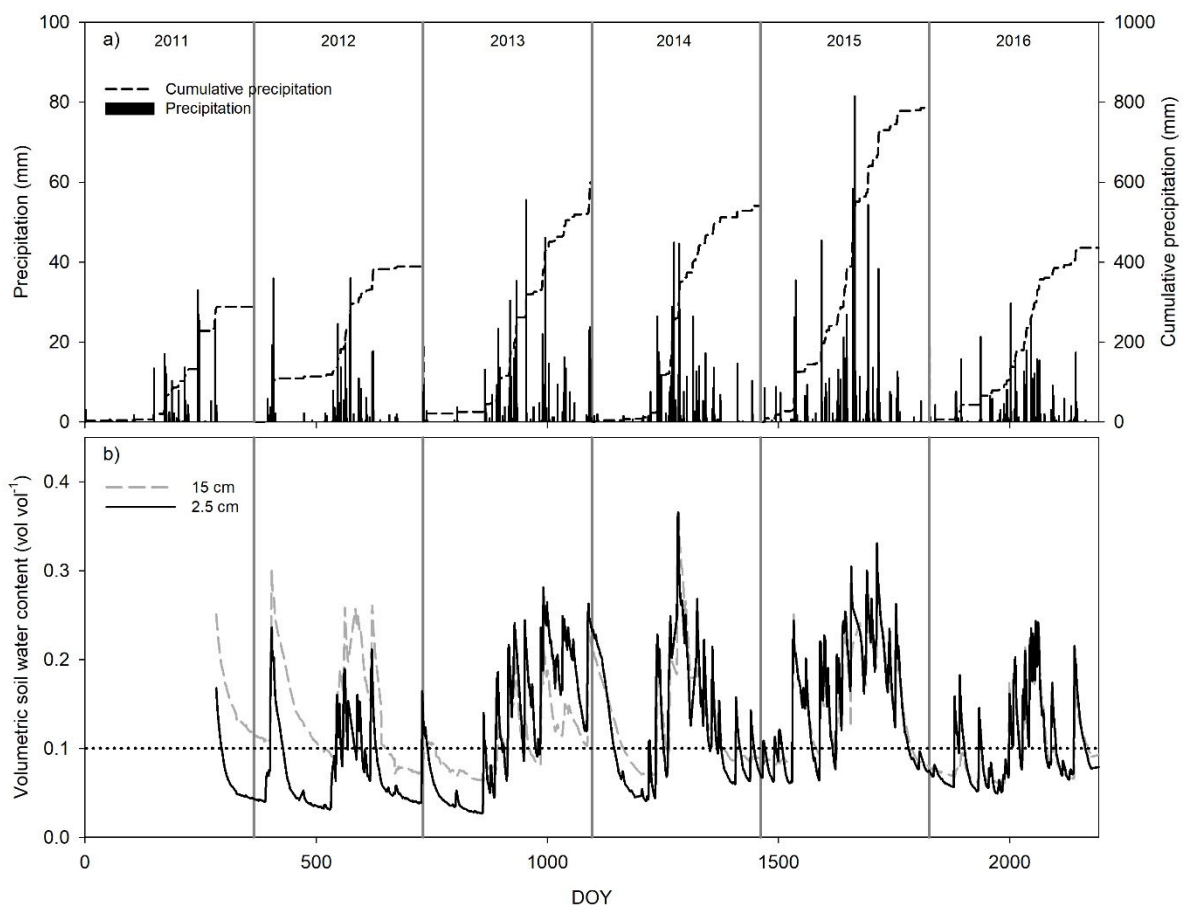
653 **Table 1. Relative importance (RI) of the first four most important environmental factors for the “priming CO₂**
 654 **effect”.**

	RI
Respiration-dominated period	
$\Delta\text{VWC}_{2.5}$	18.66
preNEE	14.67
preVWC _{2.5}	14.08
PPT	13.64
preVWC ₁₅	8.09
VWC _{2.5}	7.46
Photosynthesis-dominated period	
preNEE	33.32
VWC ₁₅	12.25
ΔPPFD	11.52
VWC _{2.5}	9.16
Tair	8.32
preVWC _{2.5}	7.79

655

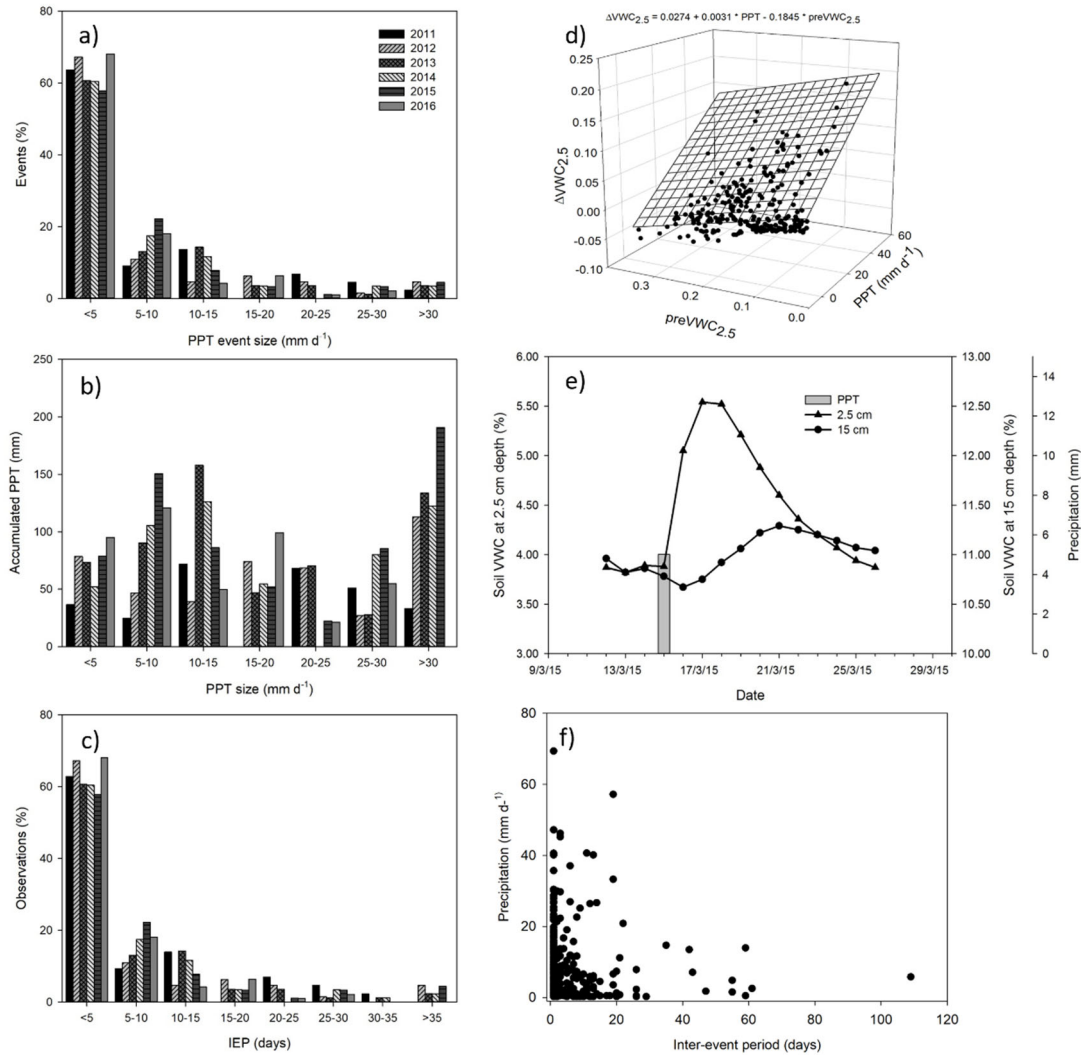
656

657



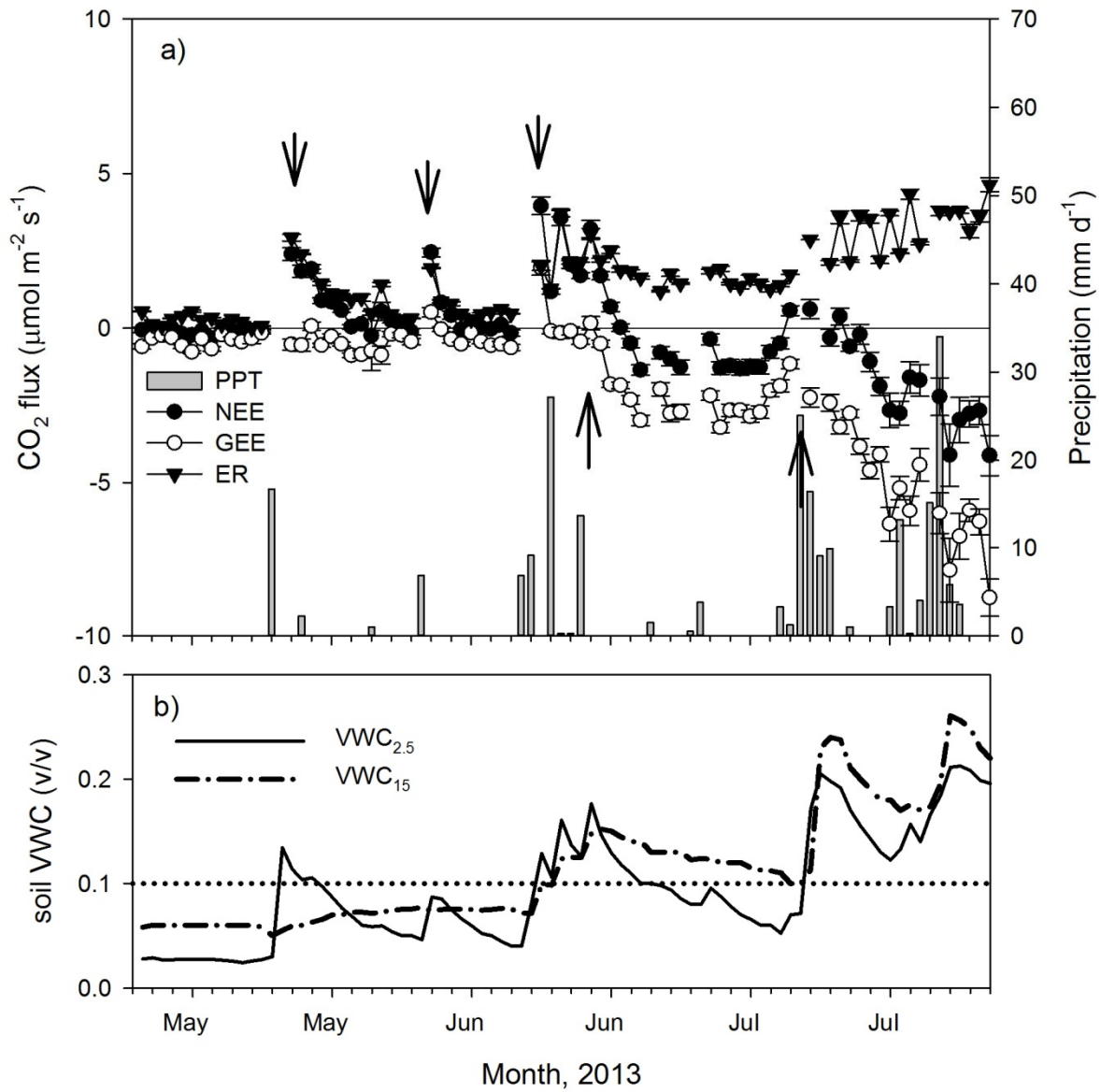
658

659 **Figure 1. Seasonal and interannual variation of daily precipitation and cumulative precipitation (a), and volumetric**
 660 **soil water content at 2.5 (black line) and 15 cm depth (gray line; b). Dotted line at 10% of soil ~~water~~was content was**
 661 **depicted as reference.**



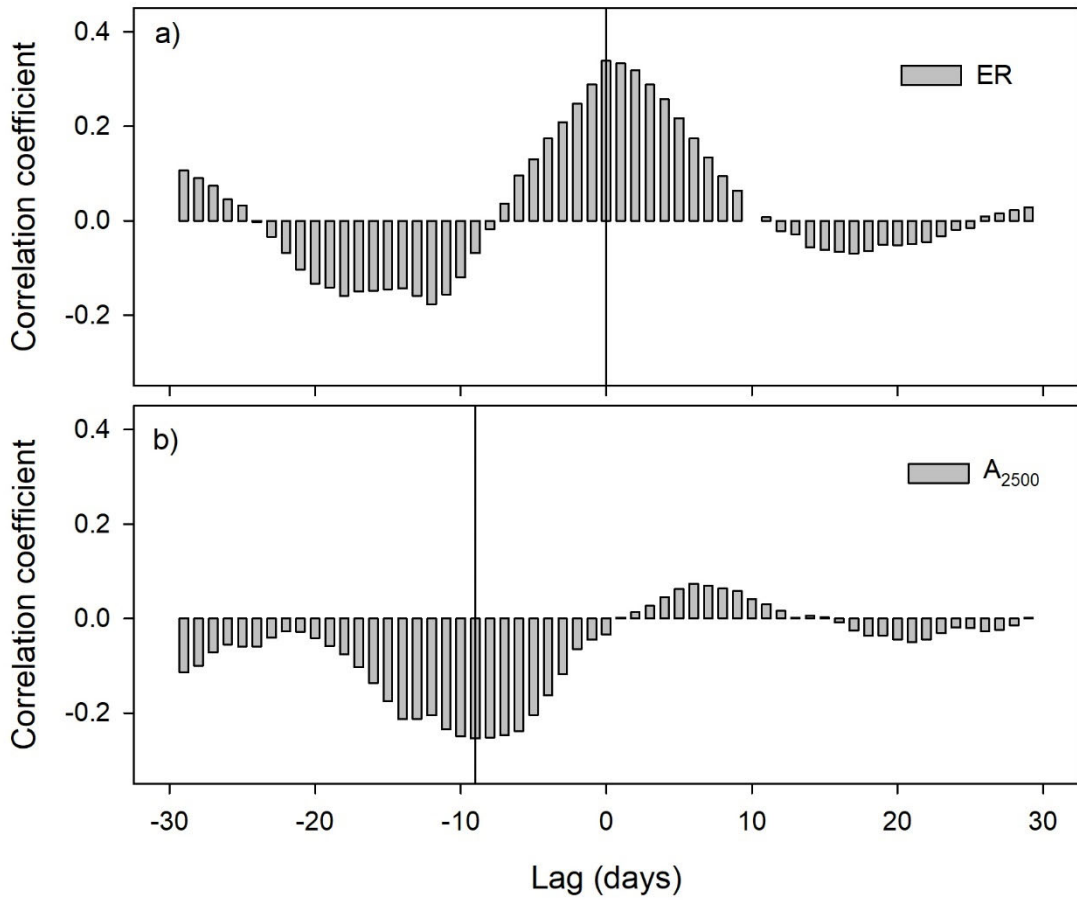
662

663 **Figure 2. Characterization of precipitation pattern. Histogram of the size of precipitation events through six years**
 664 **(a), the accumulated precipitation by size of precipitation event (b), and the number (%) of precipitation events by**
 665 **inter-event period classes (IEP, days; c). Relationship between size of precipitation event (mm d^{-1}), previous**
 666 **volumetric soil water content at 2.5 cm depth (v/v) and the change in soil volumetric water content at 2.5 cm depth**
 667 **(v/v). Dynamic of soil water content at two depths (2.5 and 15 cm) after a precipitation event of 5 mm through the**
 668 **time (e), and relationship between inter-event period and the size of precipitation event (f).**



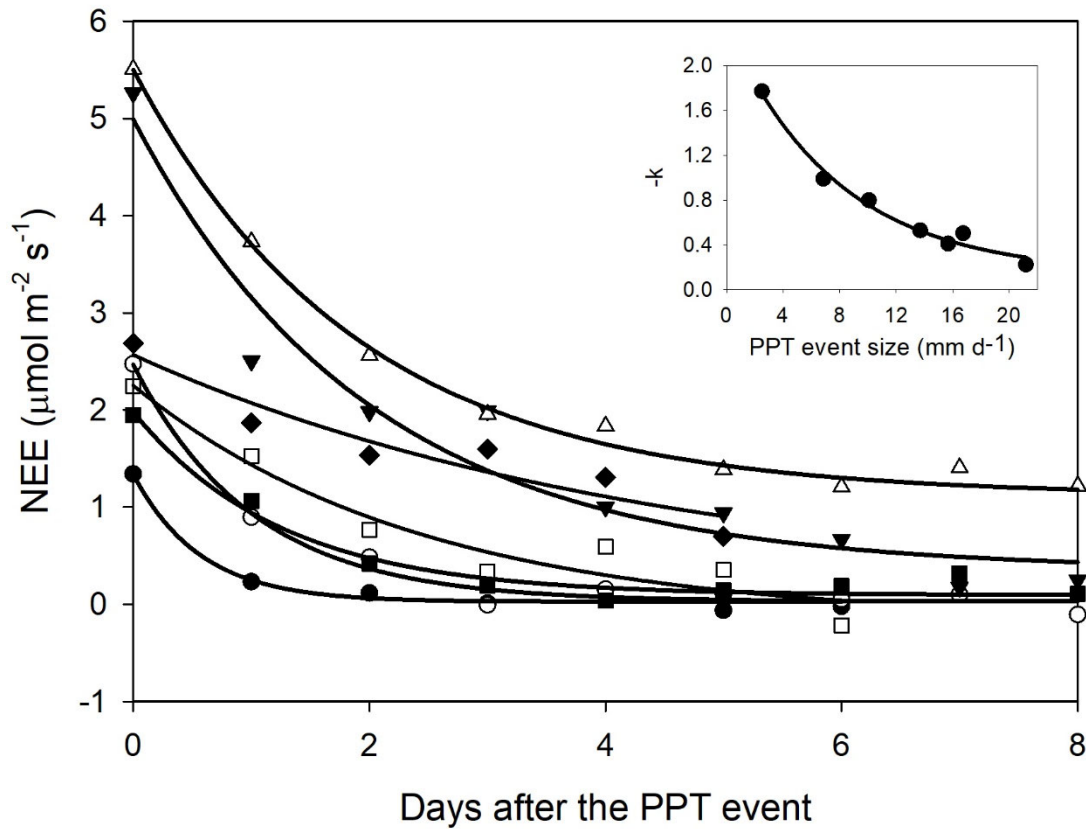
669

670 Figure 3. Dynamics of a) precipitation (mm d^{-1}) and net ecosystem exchange (NEE, $\mu\text{mol m}^{-2} \text{s}^{-1}$, daily means ± 1 SE)
 671 and its components, the gross ecosystem exchange (GEE, $\mu\text{mol m}^{-2} \text{s}^{-1}$) and ecosystem respiration (ER, $\mu\text{mol m}^{-2} \text{s}^{-1}$)
 672 for the transition from the dry (December – May) to the wet season (June – November) in 2013. b) volumetric soil
 673 water content dynamics (VWC, v/v) at two depths (2.5 cm and 15 cm). Arrows indicate apparent changes in GEE and ER trends.
 674 ~~Dotted~~The dotted line indicates SWC = 0.1.



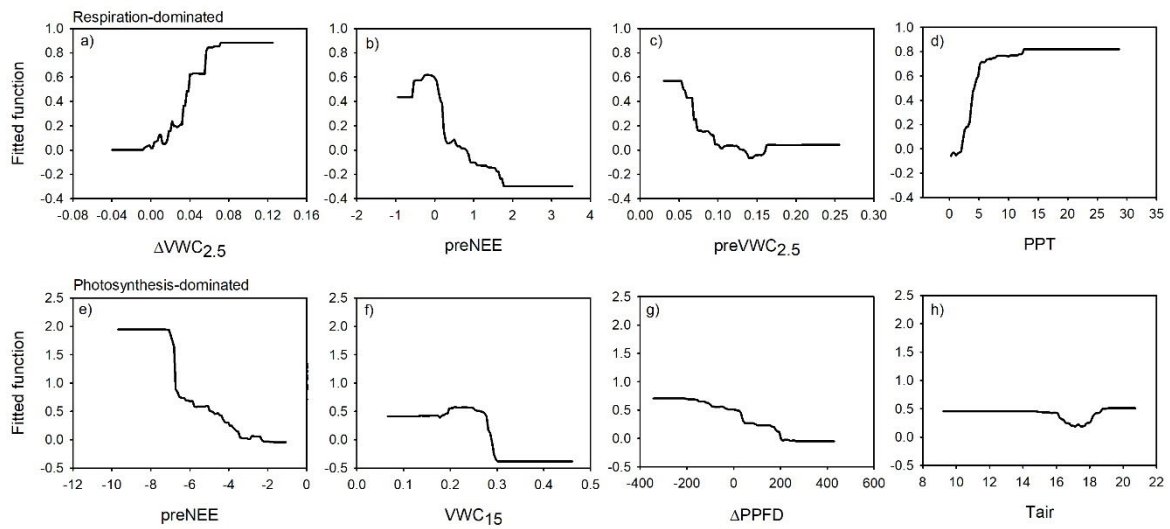
675

676 **Figure 4. Cross-correlation coefficients between detrended time series of soil water content at 2.5 cm depth and**
 677 **ecosystem respiration (ER, a), and between soil water content at 15 cm depth and photosynthesis at 2500 $\mu\text{mol m}^{-2}$**
 678 **s^{-1} of photosynthetic photon flux density (A_{2500} ; b).**



679

680 Figure 5. Net ecosystem exchange (NEE) after a precipitation event showing the decreasing effect through time
 681 (days). The decreasing effect rate was adjusted to an exponential negative model $NEE = y_0 + a \cdot \exp(-k \cdot t)$. The
 682 insert stands for the relationship between the decaying rate ($-k$) and the PPT event that originated the NEE change.
 683 This relationship was fitted with an exponential model (black line; $-k = y_0 + a \cdot \exp(-b \cdot \text{PPT_event})$). Symbols indicate
 684 different PPT event sizes that originated the NEE change, 13.7mm d⁻¹ (Δ), 16.74 mm d⁻¹ (\blacktriangledown), 6.86 mm d⁻¹ (\circ), 10.08
 685 mm d⁻¹ (\blacksquare), 2.52 mm d⁻¹ (\blacklozenge), 21.18 mm d⁻¹ (\square), and 15.68 mm d⁻¹ (\blacklozenge), (\bullet).



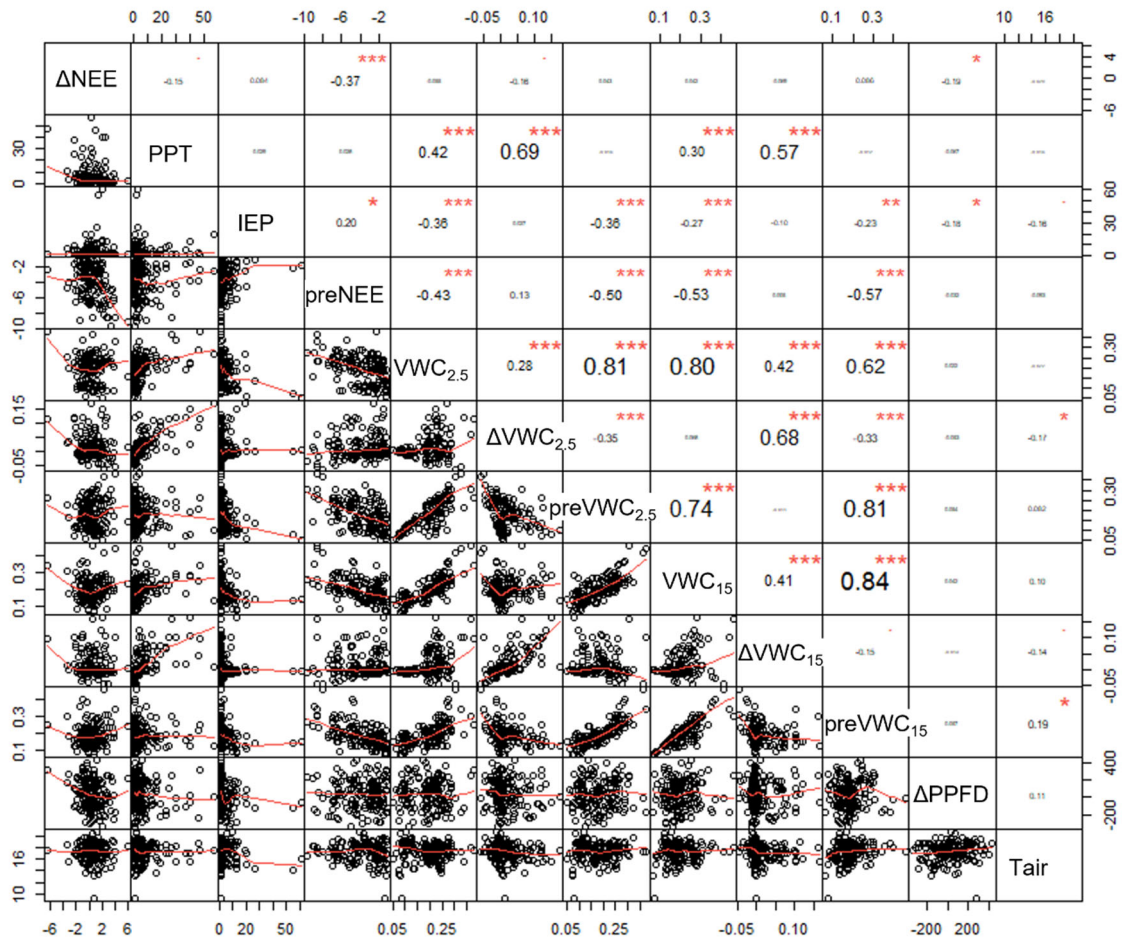
686

687 **Figure 6. Fitted functions of the boosted regression trees between the “priming CO₂ effect” and the four most**
 688 **important environmental variables at ecosystem respiration-dominated period (upper panel) and at the**
 689 **photosynthesis-dominated period (bottom panel). Priming effect (ΔNEE , $\mu\text{mol m}^{-2} \text{s}^{-1}$); previous NEE (preNEE, μmol**
 690 **$\text{m}^{-2} \text{s}^{-1}$); previous VWC at 2.5 cm depth (preVWC_{2.5}, v/v); PPT event size (PPT, mm); VWC at 15 cm depth (VWC₁₅,**
 691 **v/v); change of photosynthetic photon flux density ($\Delta PPFD$, $\mu\text{mol m}^{-2} \text{s}^{-1}$); air temperature (T_{air}, °C).**

692

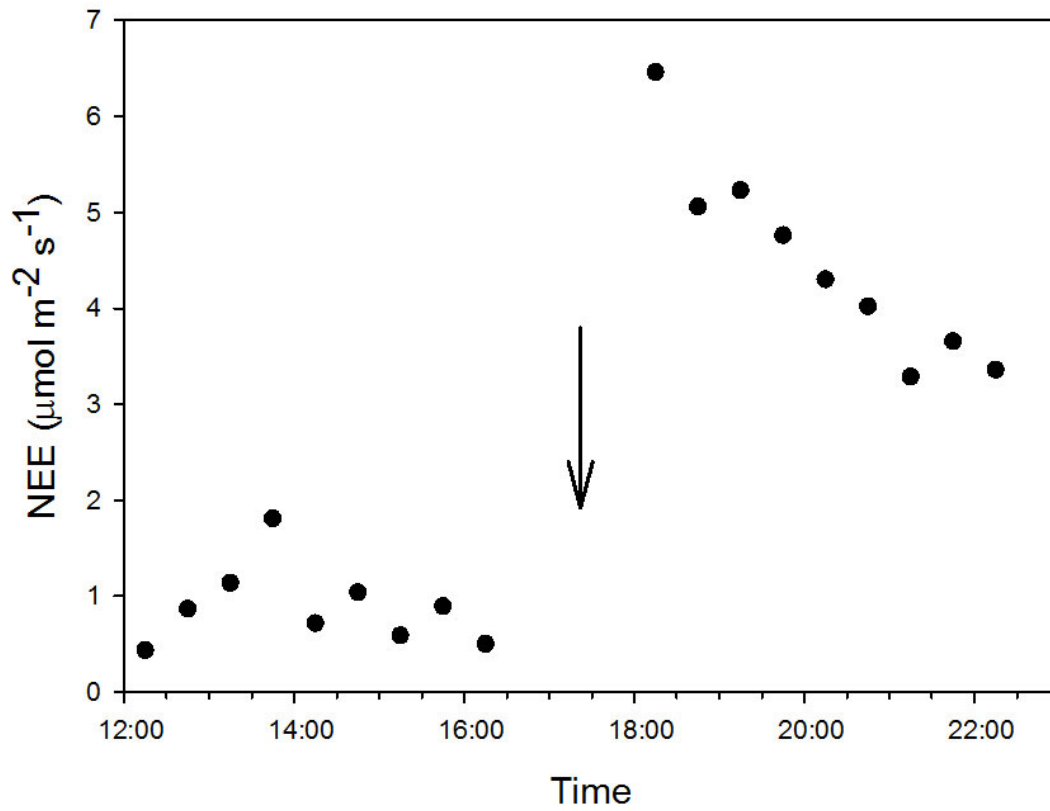
693

705 to smaller size PPT events than GEE, therefore, small PPT events favor C release whereas large PPT events
706 stimulate net C uptake by the ecosystem. Differences of time responses between soil microorganisms and plants
707 to soil wet up led GEE and ER to differ in time delays (τ), with shorter time delays for ER than GEE (Huxman
708 et al., 2004a). The hypothetical curve for NEE and its components was calculated introducing arbitrary
709 parameters in the T-D model equations of Ogle and Reynolds (2004).



710

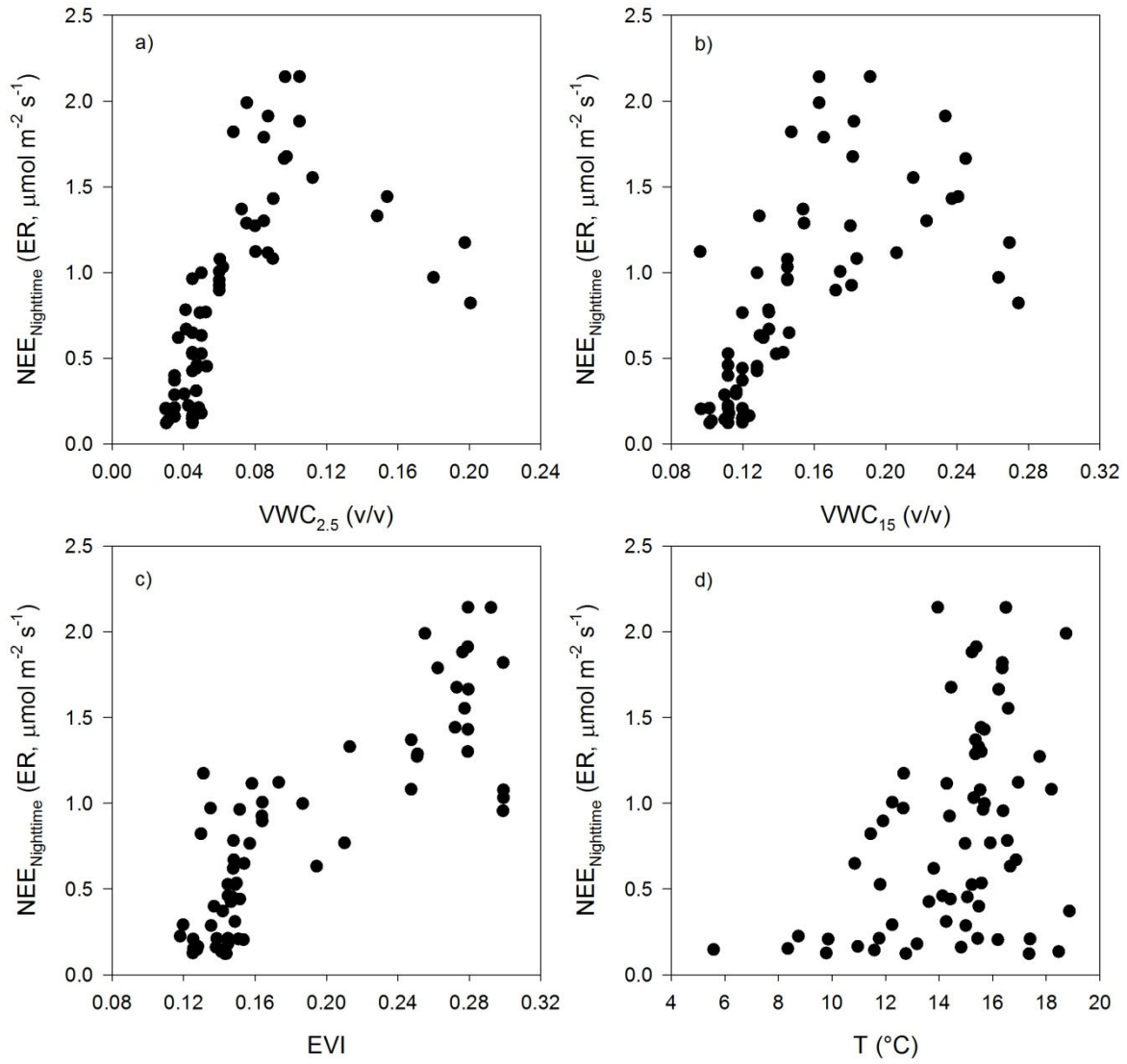
711 **Figure A2.** Correlation matrix among all variables.



712

713 **Figure A3.** Dynamic of half an hour net ecosystem exchange ($\mu\text{mol m}^{-2} \text{s}^{-1}$) after a precipitation event of 8.12

714 mm. The arrow indicates the time of PPT event occurrence.



715

716 **Figure A4.** Relationship between nighttime-NEE derived ER and a) the soil volumetric water content at 2.5 cm
 717 depth ($VWC_{2.5}$, v/v), b) the soil volumetric water content at 15 cm depth (VWC_{15} , v/v), c) the enhanced
 718 vegetation index (EVI), and d) the air temperature (T , $^\circ\text{C}$).